

Energy Reduction Methods in the Aeration Process at Perth  
Wastewater Treatment Plant

Murray A. Henderson

## Acknowledgements

Special thanks to the following people:

Jacqueline Wilkie, Albero Sanchez, Vidar Larsen, Mathew Wade, Reza Katebi, and Gavin Doo.

## Abstract

The aim of this research was to provide some degree of insight into the problem of energy overuse in the activated sludge process. The ASM1 model was used to describe the changes in levels of dissolved oxygen in three aeration “compartments”, each containing one mechanical aerator at the wastewater treatment plant at Perth, Scotland. Process parameters such as tank volumes and recycle rates were provided along with one week of telemetry data giving influent flowrates, and MLSS and DO concentrations in each aeration lane. The energy expenditure, and resultant cost were considered for the existing set up and for a number of process alternatives including PID control, variable speed drives and the installation of diffused aerators.

*Key words: dissolved oxygen control, activated sludge process, energy management*

## Contents

Aims	5
Chapter 1- Background	
Overview of Perth Wastewater Treatment Plant	7
The Activated Sludge Process	8
The polluting strength of wastewater	10
Monod Kinetics	11
Chapter 2 – Modelling of the Activated Sludge Process	
IAWQ notation and ASM1 matrix	12
IAWQ components	14
Description of original COST model	17
Influent Filtering	18
Mass Balances	20
Influent Normalisation	22
Description of Perth WWT model	23
Aeration System	28
Constant flow simulations	33
Telemetry flow simulations	37
Chapter 3 –Control of the Activated Sludge Process	
Introduction to control	39
On-Off Control	40
PID Control	44
Diffused Aeration	50
PID control of Diffused Aeration	55
Chapter 4 – Discussion and Conclusion	
Cost of Each Mode of Aeration	58
Table of Relative Projected Annual costs	62
Conclusion	63
Further Work	65
Appendices	66
Bibliography	86

## Aims

To model the Perth WWT plant activated sludge process, with telemetry data from the plant.

To implement control systems and comment on their viability.

To compare mechanical and diffused aeration

To give estimations of the relative running cost of each system.

## Introduction

Energy management as a concept originated from the 1973 Arab Oil Embargo, and since then it has grown as a money saving approach for many businesses, aided by both the environmental and political concerns about limitations in the supply and trade of oil and the impact of power generation and energy utilisation on the environment. The practice is applied to all sectors of the economy, though not always successfully, in order to bring about reductions in energy use and the ultimate goal of energy independence.

In the case of Waste Water Treatment, the Activated Sludge Process is the most energy intensive. Subsequent to a preliminary energy audit, telemetry data from the Wastewater treatment plant in Perth, Scotland showed the process of aeration of Activated Sludge consuming some 40-50% of the total energy use for the plant. A further study into the specific energy consumption, e.g. energy consumption per unit volumetric flow, found that the works was wasting energy operating the aerators at the same rate during periods of reduced load. There was no control system regulating aeration to the tank.

This project aims to describe methods of energy reduction specific for the Activated Sludge Process. Flow data from the Perth Wastewater Treatment Plant along with the computer modelling package MATLAB/Simulink™ will be used to describe process characteristics at the Perth plant. The report will investigate energy saving alternatives specific to the Activated sludge process at the plant, in order of increasing cost, and will introduce the concept of process control to the Activated Sludge process.

## Chapter 1. Background

### 1.1 Overview of Perth Wastewater Treatment Plant.

The activated sludge process is the most complex process in most Waste Water Treatment (WWT) plants, as it involves the reduction or removal of the organic portion of the waste by bio-reaction, or the digestion by a specialised culture of micro-organisms within the tank. Other processes, for example screening, grit removal and primary and final sedimentation, are largely physical. However a brief description of the overall WWT process is necessary to consider the role of the Activated Sludge Process.

Preliminary Treatment involves screening and grit removal. In the Perth Wastewater Treatment Plant, the raw sewage is discharged through a set of “Archimedes Screw” pumps, then flows through a screen inlet channel and is directed onto a mechanical screen. Debris exceeding 3mm in size is collected and removed mechanically into a common discharge channel. The screenings are then washed in a screw conveyor and then pressed by a compactor. Grit Removal occurs in a single detritor, where heavy grit particles are allowed to gravity settle whilst lighter organic solids remain in suspension and pass through.

The final stage of primary treatment is the initial settling, occurring in three large sedimentation tanks.

Secondary treatment involves the Activated Sludge Process and final sedimentation. In the Perth WWT plant, the activated sludge influent flow is split in penstocks into three long and thin aeration tanks arranged in parallel, each with three mechanical aerators. The influent stream and returned sludge enters at one end and the treated effluent leaves at the other. From here the flow is directed into three final settling tanks, one for each activated sludge aeration lane. Particles from the bioreactors are then separated by gravity and fall to the bottom of the tank, where they are directed by radial scrapers into a central hopper. A portion of this flow is recycled back to the aeration tank and the remainder is wastage flow, or WAS. Lime is then added to a portion of the WAS sludge so that it can be used as farm fertiliser, the rest becomes waste for landfill.

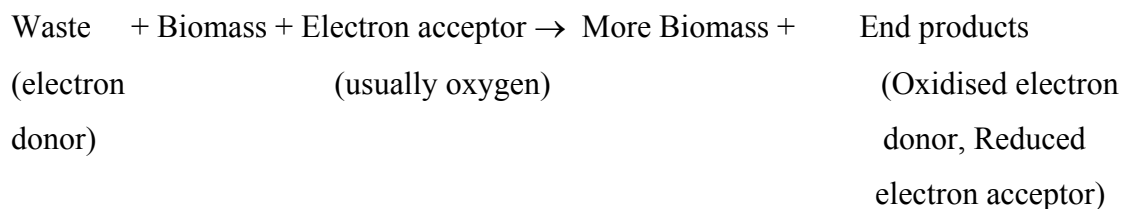
## 1.2. The Activated Sludge Process

The activated sludge process involves secondary biological treatment where residual concentrations of carbon are reduced to levels below consent standards. The biological treatment of wastewater reduces water pollution impact by reducing the bacterial energy source prior to discharge into receiving waters. The process prevents excess growth of bacterial populations in the receiving water, which in turn prevents oxygen removal and its associated environmental problems.

However, the bacterial concentration in the influent flow is weak and has to be maintained by a constant recycle of sludge from the final settler to the aeration tank. This feed is known as the RAS (recycle aeration stream) and the sludge (micro-organism) retention time is controlled by manipulation of the RAS flow.

The basic function of an activated sludge process is to convert biodegradable substrate to new bacteria cells, known as biomass, carbon dioxide and water by the process of respiration.

The respiration of micro-organisms in the activated sludge tank can be represented by the general equation\*:



\*provided proper environmental conditions.

The biomass present in the activated sludge process is a diverse population of micro-organisms including bacteria, yeasts, moulds, protozoa, rotifers, worms and insect larvae. However, for simplicity the concentration of these micro-organisms is referred to as the concentration of biomass or mixed liquor suspended solids. (Energy in wastewater treatment, Owen p70) The energy requirements for the activated sludge process are determined almost entirely by the by the oxygen demand. In mechanical aeration, where oxygen is introduced into the tank by violent agitation of the sludge mixture, the energy costs far outweigh settler operations and RAS pumping. The



amount of oxygen consumed in the process is estimated by a COD balance, where the oxygen concentration is given units of negative COD per unit mass according to the principle of continuity. (IAWQ ASM1 report) In other words when oxygen diffuses into the tank, the COD load of the activated sludge mixture reduces. However, dissolved oxygen concentrations above  $2\text{mg}(\text{COD}/\text{O}_2)/\text{l}$ , are wasteful due to the cell metabolism of the biomass. Additionally, a saturation value for dissolved oxygen of around  $8\text{mg}/\text{l}$  means that there are diminishing returns on oxygen diffusion as aerator power is increased. Indeed, as will be shown later, the Perth WWT telemetry data shows dissolved oxygen concentrations approaching this saturation value over a relatively short period of time. This represents inefficient energy use in the aeration process.

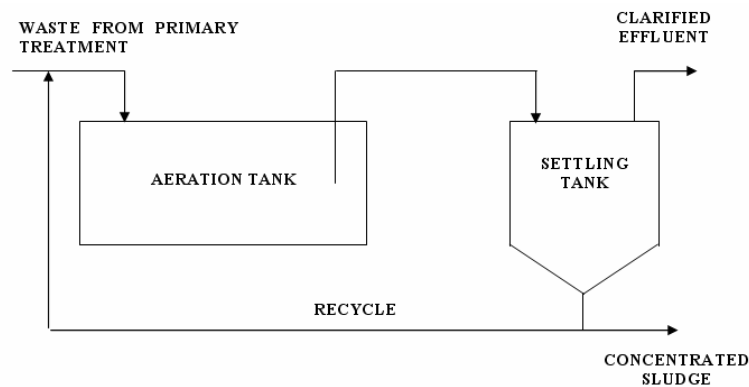


Figure 1.1: Activated Sludge Process

In addition to carbon removal, modern wastewater treatment plants reduce levels of ammoniacal nitrogen and “total nitrogen” through the processes of nitrification and denitrification respectively. Ammoniacal Nitrogen levels in domestic sewage are relatively high (around  $20\text{mg}/\text{l}$ ) which is usually above consent standards of around  $15\text{mg}/\text{l}$ . (Larsen) The removal of ammoniacal nitrogen occurs in oxygen free tanks before the aeration process. The breakdown of Ammoniacal Nitrogen occurs during “aerobic growth of heterotrophs and autotrophs” and “anoxic growth of heterotrophs” (Henze et al). By definition, organisms which use organic cell carbon for the formation of cell tissue are *heterotrophs*, whilst organisms that derive cell carbon from carbon dioxide are *autotrophs*. In modern modelling techniques, the biomass concentration is divided into autotrophic and heterotrophic bacteria, since they have different effects on state concentration within the tank.

Heterotrophic bacteria are utilised in the anoxic part of the activated sludge process, where denitrification occurs. This involves the conversion of nitrates to nitrogen gas. Nitrification occurs in the aerated activated sludge tanks(s) by the oxidation of ammonia to nitrate. This nitrate is then used as the terminal oxygen acceptor for the denitrification process, thus the two processes are linked.

The disadvantages of this method are that the COD load is greater at the influent end of the tank and thus the oxygen concentration here is less. There is therefore a decreasing oxygen gradient along the length of the tank in long thin plug flow systems such as this. (Larsen)

### 1.3. Measurement of the Polluting Strength of Wastewater.

The “polluting strength” of wastewater is measured by a number of different factors, most notably the Biochemical Oxygen Demand (BOD) and Chemical Oxygen Demand (COD). Both measure the oxygen equivalent of that sample of wastewater, or the amount of oxygen that would be removed from receiving waters if the sample was released to the environment. Other methods for measuring the strength of wastewater have been developed but they are not in widespread use in the industry. (Metcalf)

#### 1.3.1 BOD

The biochemical oxygen demand (BOD) is defined by the quantity of oxygen required for the complete oxidation of bio-degradable matter, present in a wastewater sample by the aerobic action of micro-organisms. This can be expressed in two forms, the 5-day biochemical oxygen demand ( $BOD_5$ ), which is taken over a period of 5. The second is the ultimate biochemical oxygen demand ( $BOD_U$ ) where a measurement is taken until there is no further increase in oxygen consumption. (Grady Jnr)

#### 1.3.2 COD

The chemical oxygen demand, by contrast, measures the organic matter present in the waste which can be oxidised by a strong chemical oxidising agent, such as Potassium Dichromate, in an acidic medium. Although the COD is not used as widely as BOD, the COD is used more in mathematical modelling of the activated sludge process because it provides a link between electron equivalents in the organic substrate, the biomass and the oxygen utilised. (Henze et al)

## 1.4. Description of Monod Kinetics

The exponential nature of bacterial growth is described by Monod kinetics, which specifically states that the rate of growth of a bacterial population depends on the concentration of one or more limiting nutrients. That is the concentration of any factor (substrate, oxygen, nitrogen) required for the growth of the bacteria. The effect of such a limiting factor on cell growth is described by the Monod expression:

$$\mu = \mu_m \cdot \frac{S}{K_s + S}$$

where:

$\mu$  = specific growth rate,  $\text{time}^{-1}$ ,

$\mu_m$  = maximum specific growth rate,  $\text{time}^{-1}$ ,

$S$  = concentration of growth limiting substrate in solution, mass/unit volume

$K_s$  = half velocity constant, substrate concentration at one half the max growth rate, mass/unit volume.

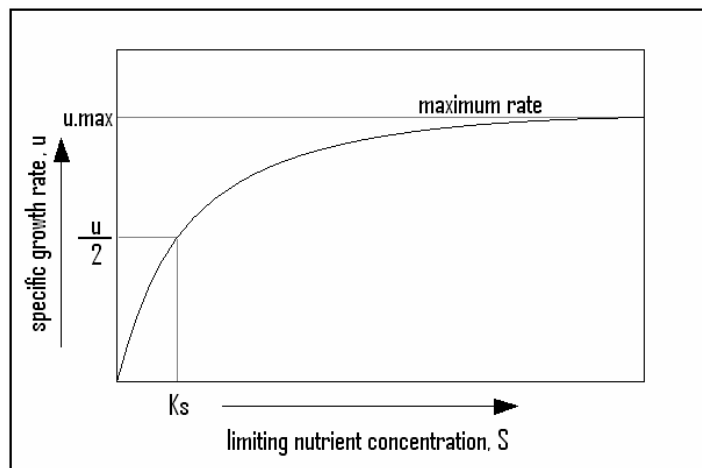


Figure 1.2: Effect of a limiting nutrient on the specific growth rate

As can be seen from the above figure, as the substrate concentration is increased,  $\mu$  initially rises rapidly, but then asymptotically approaches a maximum, the maximum specific growth rate. The term  $K_s$  describes the rate at which  $\mu$  approaches  $\mu_m$ . The smaller it is, the lower the substrate concentration which corresponds to  $\mu_m$ . Monod kinetics, as described by the above equation is central to any mathematical description of the growth of biomass in an activated sludge process.

## Chapter 2: Modelling of the Activated Sludge Process.

### 2.1 Introduction of IAWQ notation and the Activated Sludge Model 1.

In this report, notation of all parameters and conditions shall be described by the standard IAWQ notation, and the basis of the aeration and activated sludge process shall be the ASM 1 model (Henze et al).

There will follow a short description of the notation itself, then a description of the mechanisms involved in the breakdown of biological substrate within the activated sludge process.

The ASM 1 model was first published in the IAWQ Scientific and Technical Report No. 3 in 1987 and since its publication it has become the most widely used activated sludge model, providing an effective basis for all new model development. There has been a recent acceleration in general understanding of the process since then, aided by the increase of computing power and the standardisation of language and notation. Continued research has resulted in the development of models ASM 2, ASM 2d and ASM 3. These models have offered considerable improvements on the original by incorporating more fractions of COD to accommodate new experimental observations (Sollfrank and Gujer 1995), by describing the growth and population dynamics of floc forming and filamentous bacteria (Gujer and Kappeler 1992) and perhaps most importantly by including new processes for the description of phosphorus removal (Henze et al).

Despite these improvements the ASM 1 model is still in the most widespread use across the world. For the purposes of this project the model provides an accurate description of the overall activated sludge process.

### 2.2 Description of Standard IAWQ notation and ASM 1 matrix

Fundamental to the description of the activated sludge process is the continuity principle which states that any component entering the system must either pass through the system, remain in the system or be destroyed in the system.



rates are determined by summing each column through  $j$  for each component, multiplying each stoichiometric coefficient with the corresponding process rate for the row. Where a stoichiometric coefficient is negative the component is consumed in the corresponding reaction and where a box is empty, the stoichiometric coefficient  $v_{ij}$  is taken as zero and the component is neither created nor consumed in the process. For example, since there are no entries listed under  $X_I$  (inert particulate organic matter) this component is deemed to be unaffected by any process in the biochemical reactor. These conversion rates are considered the output of the model and are expressed in units of concentration per unit time. E.g. g COD  $m^{-3}day^{-1}$ . The model then calculates the final component concentrations by integrating each component differential equation according to the time given for the model. These rates of change of the specific components are calculated by first assuming that over the period of 250 days the concentration of each component has changed from 0 to the final amount, after the cessation of the model. The observed conversion rate ( $di$ ) is not the change in concentration over the 250 days but rather the change in concentration from 0 gCOD/ $m^3$  to the final amount. i.e. assumption at time = 0, concentration of component  $i = 0$ .

Example:

According to the ASM 1 matrix (Appendix 2) the reaction rate of  $X_s$  (slowly biodegradable substrate) is given by:

$$r_4 = (1-f_p)b_H \cdot X_{B,H} + (1-f_p)b_A \cdot X_{B,A}$$

where

$b_H$  is the specific decay rate for heterotrophic bacteria

$b_A$  is the specific decay rate for autotrophic bacteria

$f_p$  is the fraction of biomass to particulate products

e.g slowly biodegradable substrate is formed in the bioreactor by the decay of both heterotrophic and autotrophic bacteria according to the dimensionless parameter  $f_p$ .

### 2.3 Components in the IAWQ Reactor

From the above description of the ASM 1 matrix, it can be seen that sludge floc can be broken down into a number of components whose concentrations continually vary

with time, each either being destroyed or created by a combination of several processes. The following will discuss each component and how each concentration changes over time and refers to Appendix 2 – The ASM1 matrix (Henze et al).

Firstly, components 1 and 3, representing soluble and particulate inert organic matter, undergo no chemical processes in the activated sludge process. However, they are still important parts of the model itself because they represent a fraction of the overall COD load.

The biomass concentration changes according to Monod kinetics and many of the process rates expressed in the right hand side of the matrix are Monod type growth expressions, but the growth of the microbial culture is now seen as cyclical in nature. A proportion of the dead bacteria cells are considered as slowly biodegradable substrate which can be utilised by live biomass for cell functions. Decay of biomass also results in the creation of inert particulate products. Slowly biodegradable biomass is removed from suspension instantaneously by inclusion into the sludge floc. There it undergoes conversion into readily biodegradable substrate. For the purpose of the model, the complex set of reactions responsible are considered to be one hydrolysis reaction.

Therefore, the concentration of readily biodegradable substrate ( $S_S$ ) is reduced by the growth of biomass as the biomass utilise the substrate for cell functions and also generated by hydrolysis of slowly biodegradable organic matter entrapped in the biofloc.

The process is shown more clearly in column four, where the concentration of slowly biodegradable substrate is seen to increase by the process of biomass decay, but also seen to decrease by “hydrolysis of entrapped organics”.

The columns where  $i=5$  and  $i=6$ , represent the concentration of biomass in the system, with  $X_{B,H}$  denoting heterotrophic biomass and  $X_{B,A}$  denoting autotrophic biomass. Heterotrophic bacteria is formed by aerobic and anoxic growth of biomass and destroyed by decay according to the Monod growth expressions and the decay constant in the process rate column. Growth of autotrophic biomass only occurs under aerobic conditions.

The seventh column contains the concentration of particulate products arising from biomass decay, i.e. the portion of dead suspended inert biomass which cannot be considered as slowly biodegradable substrate or live bacteria cell mass. The model describes this portion of the tank volume as being created by decay but not destroyed

by any other process. In reality however, this fraction of biomass is probably not inert to biological attack (Obayashi and Gaudy, 1973) but has a rate of destruction low enough to be considered negligible for sludge retention times normally associated with the activated sludge process.

Column eight contains the dissolved oxygen concentration,  $S_o$ , the first of two electron acceptors in the process. Not surprisingly changes in dissolved oxygen concentration are brought about by aerobic growth of biomass, as the cells utilise oxygen for respiration and as the biomass grows dissolved oxygen is taken out of the system. The 4.57 constant in the autotrophic growth process stoichiometric term is the theoretical oxygen demand associated with the oxidation of ammonia nitrogen to nitrate nitrogen.

The other electron acceptor is nitrate nitrogen,  $S_{NO}$ , in column nine which refers to the denitrification process.  $NO$  is created during aerobic growth of autotrophic bacteria and removed during anoxic growth of the heterotrophic biomass, where nitrate nitrogen is converted to nitrogen gas in the absence of oxygen. Although nitrate nitrogen is an intermediate formed during nitrification, for simplicity it is assumed the nitrate is the only oxidised form of nitrogen present. The 2.86 constant in the stoichiometric coefficient for the “anoxic growth of heterotrophs” process is the oxygen equivalence for conversion of nitrate nitrogen to nitrogen gas ( $N_2$ ) and is included to maintain consistent units.

The tenth column contains “soluble ammonia nitrogen”  $S_{NH}$ , assumed to be the sum of the ionized (ammonium) and unionized (ammonia) forms. However, for pH values such that would normally be experienced in the process, the unionized form is insignificant so it is sufficient to express ammonia oxidation in terms of the total ammonium nitrogen concentration. Ammonia nitrogen is formed by ammonification of soluble biodegradable organic nitrogen and is removed by growth of the biomass. Most of this component is utilised as the energy source for aerobic growth of the autotrophic biomass. The column also provides a term for the nitrogen incorporated into the biomass during cell synthesis ( $-i_{XB}$  is included for both heterotrophic and autotrophic biomass, where  $i_{XB}$  is the ratio of the mass of nitrogen to the mass of COD in biomass).

Soluble biodegradable organic nitrogen is included in column  $i=11$ , which is converted to soluble ammonia nitrogen as discussed above. The component is formed by hydrolysis of particulate organic nitrogen.



The concentration of the particulate organic nitrogen from which the soluble biodegradable organic nitrogen is formed is expressed in column twelve ( $i=12$ ). It is also generated by decay of heterotrophic and autotrophic organisms,  $i_{XB}$ , minus the amount associated with the inert particulate products  $f_{pi_{XP}}$ .

The  $i=13$  column, although not essential to the model, represents total alkalinity,  $S_{ALK}$ . This component is included to provide information whereby undue changes in pH can be measured.

The components discussed represent the minimum required to model effectively the entire activated sludge process, however the most important component for this model is the dissolved oxygen concentration. Other components which have no effect on its concentration are included in the final model only as indicators of the effectiveness of the model.

## 2.4 Description of Original Model

As previously discussed, the ASM 1 was developed in 1987 and has since become widely utilized for control of activated sludge, particularly in the aeration process.

More recently, a publication by the “COST” symposium, on behalf of the European commission, made the ASM1 more accessible to wastewater treatment plant engineers. The “COST simulation benchmark” was produced as a result of a co-operation by several contributing authors and focussed on biological wastewater treatment processes and the optimisation of their design.

The final result was a full description of activated sludge simulation protocol and a tool for “evaluating activated sludge wastewater control strategies”.

The publication contains instructions on the design and control of a wastewater treatment plant using a number of software programmes including MATLAB/Simulink™, and contains the complete mathematical description of the ASM 1 model in C notation for inclusion in Simulink.

This publication was used as the starting point in the modelling of the Perth Wastewater Treatment Plant activated sludge process.

The original COST simulation benchmark model differs in a number of ways from the activated sludge process at the Perth WWTP. Appendix 3 shows the Simulink™ flow diagram associated with the model. In it, there are five separate aeration tanks in series, two anoxic and three aerobic.

In the COST model oxygen is supplied by diffused aeration, a more efficient method where bubbles of air or oxygen diffuse into the sludge through a number of orifices at the base of the tank. Additionally there are two recycle streams, the RAS flow, as in the Perth process and a second internal recycle from the final reactor to the first which bypasses the final settler.

## 2.5. Filtering of Flow data from Wastewater Treatment Plant

The flow rates, MLSS and DO concentrations were provided by the Perth Wastewater Treatment Plant in the form of telemetry data. On first inspection however, the flow data appeared to contain a considerable amount of high frequency noise which were decided to have been caused by flow meter disturbances. For this reason a MATLAB™ filter function was utilised to minimise noise in the telemetry flowrate data provide a smooth curve for input into the model.

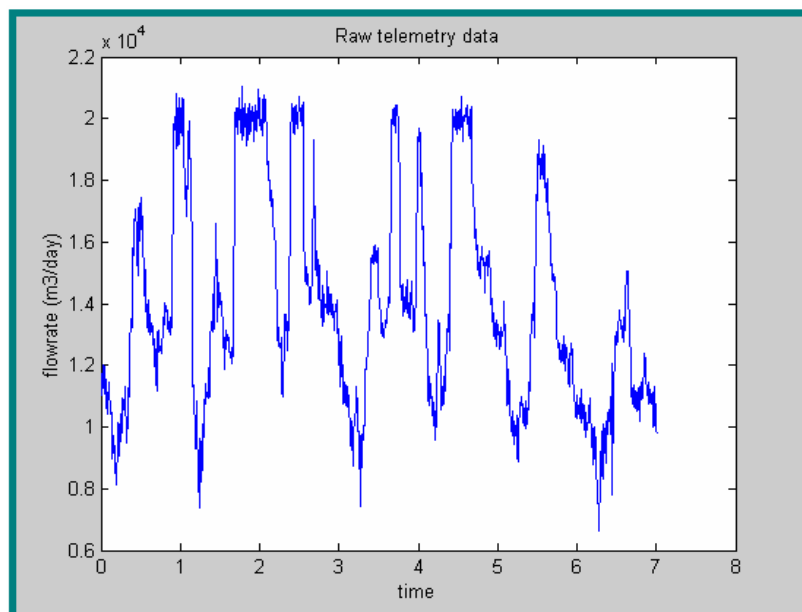


Figure 2.2: Unfiltered telemetry influent data

The MATLAB™ command “CHEBY1” creates a Chebyshev type 1 analogue filter where:

$$[B,A] = \text{CHEBY1}(N,R,W_n)$$

This designs an Nth order lowpass digital filter with R decibels of ripple in the pass band, which is then used to filter the influent data to give the influent flowrate for the model. In this instance a second order (N=2) filter was used.

Where “Wn” is the cutoff frequency:

Such that  $0.0 < W_n < 1.0$ ,

If 1.0 corresponds to half the sample rate.

R=0.5, as recommended by the MATLAB™ help function.

The command “FILTER” is then used to filter the flow data in vector “telemetryflow” with the “chebychev” filter described by vectors B and A to create the filtered data “filteredflow”.

e.g `filteredflow = FILTER(B,A,telemetryflow)`

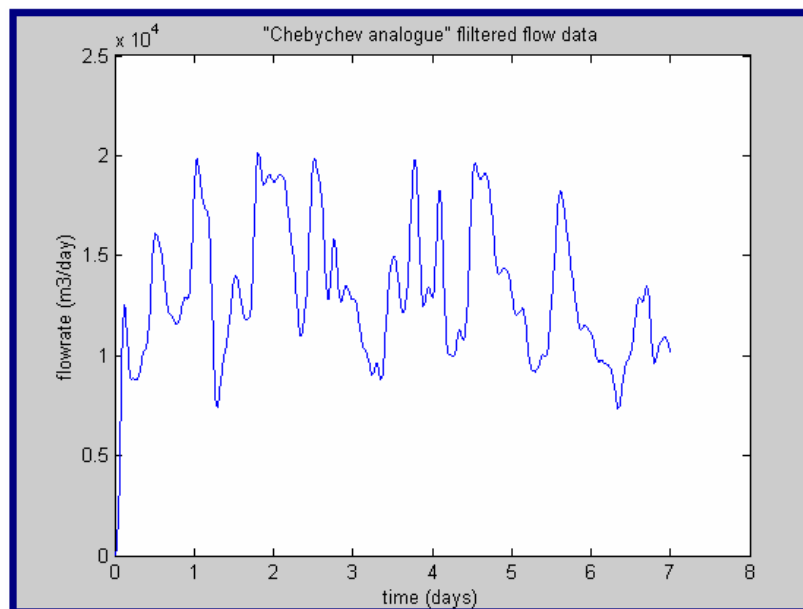


Figure 2.3: Filtered flow data

## 2.6 Initial Mass Balance.

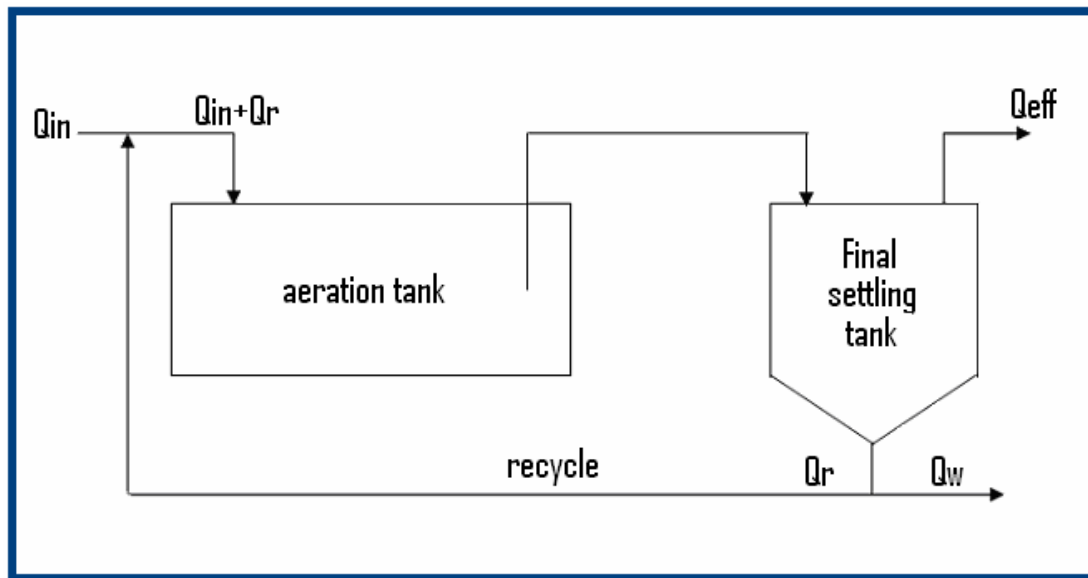


Figure 2.4 – Flow diagram of Activated Sludge Process.

A mass balance provides flow information at all stages of the activated sludge process. The influent rate given from telemetry data for the inflow rate:

$$Q_{IN} = 13990.68 \text{ m}^3/\text{day}$$

Where  $13990.68 \text{ m}^3/\text{day}$  is the average flow of the influent to the bioreactor from telemetry data.

Tank dimensions: 10.7m square, 4m depth.

Volume of each tank, in which there are 3 compartments in each lane, from plant data:

$$\begin{aligned} \text{Reactor volume} &= 10.7\text{m}^2 * 4\text{m} * 3 \\ &= \underline{1373.88\text{m}^3}. \end{aligned}$$

Reactor Capacity is given as  $400\text{m}^3$

From data given by Perth Wastewater Plant:

$$\begin{aligned} \text{Reactor residence time} &= 4\frac{1}{2} \text{ hours at dry weather flow (DWF)}. \\ &= \underline{0.167\text{days}} \end{aligned}$$

The DWF was recently estimated as  $20000\text{m}^3/\text{day}$  for all three aeration lanes.

Therefore:

$$20000/3 = \underline{6666.67\text{m}^3/\text{day}}$$

Tank fluid volume =  $Q_{IN}$  \* residence time

$$= 5596.27 \text{ m}^3/\text{day} * 0.167\text{days}$$

$$= \underline{1113.33\text{m}^3}$$

Less than the line capacity of 1200m<sup>3</sup>.

But, from telemetry data given by Perth Wastewater Plant:

$$Q_{IN} = 13990.00 \text{ m}^3/\text{day}$$

Therefore

$$\frac{13990 \text{ m}^3/\text{day}}{6666.67\text{m}^3/\text{day}} = 2.092$$

The telemetry flow data averages at 2 times DWF, e.g.  $Q_{IN} = 2\text{DWF}$

Telemetry Residence time =  $1200 \text{ m}^3/13990\text{m}^3/\text{day} = \underline{2.05\text{hours}}$

The RAS flow is given by

$$\text{RAS} = 1.5 * \text{DWF}$$

So

$$Q_R = 1.5 * 6666.67\text{m}^3/\text{day}$$

$$\underline{Q_R = 10000\text{m}^3/\text{day}}$$

From original “COST simulation Benchmark” model:

Wastage flow rate:

$$Q_W = 385\text{m}^3/\text{day}$$

Flow rate from “COST simulation Benchmark” model, influent flow rate:

$$Q_{IN} = 18446 \text{ m}^3/\text{day}$$

Scaling, the wastage flow rate at the plant:

$$Q_W = 385\text{m}^3/\text{day} * \frac{13990\text{m}^3/\text{day}}{18446.00\text{m}^3/\text{day}}$$

$$Q_W = \underline{292.00\text{m}^3/\text{day}}$$

Therefore:

$$Q_E = Q_{IN} - Q_W$$

$$= 13990\text{m}^3/\text{day} - 292 \text{ m}^3/\text{day}$$

$$= \underline{13698.00\text{m}^3/\text{day}}$$

## 2.7 Normalization and Prediction of Flowrate Composition

As previously discussed, the IAWQ notation describes the composition of activated sludge as 13 different states whose concentrations vary according to specified rate equations.

However, the instrumentation required to measure all 13 variables in the influent and effluent flows and in the reactor itself would be costly and unnecessary for the effective running of the plant. For this model, the only available data on the influent was its flowrate and most cases this is the only information which is known. Therefore, the assumption of values for each of the 13 states included in the ASM 1 model is one of the initial stages of the modelling process.

The flowrates and corresponding concentrations given in the original model can be used for this purpose, providing a basis for relative concentrations of components in the influent flow even though the original flowrates do not correspond to either the reactor size or sludge retention time of the Perth model.

The model influent flow contains 16 variables, the 13 asm1 states, time, influent flowrate and the total suspended solids.

Where  $T_{ss}$ , the total suspended solids is given by:

$$T_{ss} = 0.5 * (X_I + X_S + X_{B_H} + X_P)$$

To create the new variables for the 13 state variables in the new influent flow the first row of flow values from the original “DRYINFLUENT” input was used, as shown below. The following relationship was used to determine the new component concentrations:

$$\text{newconcX} = Q_{\text{new}}/Q_{\text{old}} * X_{\text{total}} * X\%$$

Thus the total conc. of all 13 initial states:

$$X_{\text{total}} = 355\text{mg/l}$$

...and the original value of Q:

$$Q_{\text{old}} = 21,477\text{m}^3/\text{day}$$

And X% given by:

$$X\% = X_{old}/X_{total}$$

So a concentration for the 13 asm1 components can be given for each new flowrate in the telemetry data.

See Appendix 3 for MATLAB™ programme “normalization”

## 2.8. Overview of Perth WWT Simulink Model

The model shown in Appendix 5 is the main Simulink™ model for the Activated Sludge process at the Perth Wastewater Treatment Plant. This is the top level of the model, presented as a flow diagram in the Simulink™ form, and the blocks represent an input or output, function, process or reaction. The arrows represent the flow of information from one block to another. The aeration tank being modelled is shown as three separate bioreactors, representing three aeration processes and three ASM1 Models (Henze et al).

### 2.8.1 Model Inputs

The inputs, shown here in blue are either flow into the plant (at the bottom of the diagram) or constant values required for the running of the plant. For example power supplied to the aeration process and the recycle rate. The aeration subsystem converts the power of the aerators to kLa, a coefficient describing the mass transfer of gas into solution in the bioreactor. This subsystem will be described in detail later.

### 2.8.2 Model Outputs

The outputs, shown in red are mostly used to send state information to the “workspace”. This means that the state concentrations and time can be manipulated and plotted in the MATLAB™ environment. Scopes are used to plot information on state concentrations over time within the SIMULINK™ environment.

### 2.8.3 Signal Dimensions

At most stages in the model, the number of states or “signal dimensions” is 15, i.e. the 13 ASM1 concentrations as discussed earlier, the  $T_{ss}$  value and the flowrate. These values are constantly changing in the dynamic model, as the activated sludge process commences and they are also subject to disturbances from the input file. Every 10 minutes, corresponding to a telemetry measurement from the Perth process, an flow “reading” is taken from the input MATLAB™ file “newinfluent.m”. This flow is added to the plant recycle, the flow of returned sludge from the settler, in the “mux” box at the bottom left hand side of the diagram.

### 2.8.4 Combiner s function

The “combiner” block is the first of four “c file s functions”, all of which contain code written in the language c that describes a function or set of processes. In the case of the “combiner”, new concentrations of all states are calculated upon the addition of the recycle flow to the inflow. The block does this by mathematical expressions written as a list of commands.

S functions simplify the flow diagram considerably since they are MATLAB™ files and are capable of providing complex mathematical relationships whilst only being shown on the flow diagram as single blocks. This is especially useful in the case of the ASM1 and settler models which would appear cluttered if their numerous functions were displayed in SIMULINK™.

In the “combiner” each new state concentration is found for the increase in flow, according to the principle of continuity. E.g the new mass flow rate is divided by the new volumetric flow rate to yield the new concentration of each state.

For example:

$$\text{New conc}(x) = [(\text{conc. of state } i * \text{inflow rate}) + (\text{conc. of state } r * \text{recycle flow rate})] / \text{total flowrate}$$

See Appendix 9 for description of combiner code.



### 2.8.5 Hydraulic Delay S function.

The function “hyddelayv2” is a c file S function which introduces hydraulic, first order type delay into the simulation.

(see Appendix 10)

### 2.8.6 ASM 1 S function.

The ASM1 s functions contain the rate expressions for all 13 IAWQ states as a series of commands. As mentioned previously, the three ASM 1 models represent the three aerators in the aeration ditch. Essentially the ASM 1 function changes the 13 IAWQ state concentrations according to the rate expressions in the IAWQ model and provides a new set of output concentrations, which can be viewed in the workspace or plotted via the scope in the flow diagram. The “vector selector” allows selection of a single state to enable it to be plotted on the scope, without other state concentrations. In this model, the dissolved oxygen concentration was plotted and compared with the oxygen concentration in the inflow to the bioreactor.

The ASM 1 c-file first defines all the kinetic parameters used in the IAWQ notation, e.g. specific growth rates, yields, decay rates and all constants in the rate expressions. See Appendix 6. The kinetic parameter values were obtained from literature. (COST Simulation benchmark)

The process rates are then given, corresponding to the expressions “ $\rho_j$ ” on the right hand side of the IAWQ ASM 1 matrix (Henze et al).

So process rate 1:

$$\mu_{mH} \left( \frac{S_s}{K_s + S_s} \right) \left( \frac{S_o}{K_{OH} + S_o} \right) X_{B,H}$$

is given in c notation as:

```
proc1=mu_H*(xtemp[1]/(K_S+xtemp[1]))*(xtemp[7]/(K_OH+xtemp[7]))*xtemp[4];
```

The parameters given the notation “xtemp[n]” as above where n=1,2...11 are the concentrations of the 13 states which appear in the ASM process rate expressions (column  $\rho_j$  in the matrix).

e.g

X temp(1.) = S<sub>S</sub>  
X temp(3.) = X<sub>S</sub>  
X temp(4.) = X<sub>B,H</sub>  
X temp(5.) = X<sub>B,A</sub>  
X temp(7.) = S<sub>O</sub>  
X temp(8.) = S<sub>NO</sub>  
X temp(9.) = S<sub>NH</sub>  
X temp(10.) = S<sub>ND</sub>  
X temp(11.) = S<sub>ND</sub>

In fact only 9 inputs are used in the process rate expressions.

The c file describes the process rates thus:

1. `proc1=mu_H*(xtemp[1]/(K_S+xtemp[1]))*(xtemp[7]/(K_OH+xtemp[7]))*xtemp[4];`
2. `proc2=mu_H*(xtemp[1]/(K_S+xtemp[1]))*(K_OH/(K_OH+xtemp[7]))*(xtemp[8]/(K_NO+xtemp[8]))*ny_g*xtemp[4];`
3. `proc3=mu_A*(xtemp[9]/(K_NH+xtemp[9]))*(xtemp[7]/`
4. `(K_OA+xtemp[7]))*xtemp[5];`
5. `proc4 = b_H*xtemp[4];`
6. `proc5 = b_A*xtemp[5];`
7. `proc6 = k_a*xtemp[10]*xtemp[4];`
8. `proc7=k_h*((xtemp[3]/xtemp[4])/(K_X+(xtemp[3]/xtemp[4])))*((xtemp[7]/(K_OH+xtemp[7]))+ny_h*(K_OH/(K_OH+xtemp[7]))*(xtemp[8]/(K_NO+xtemp[8])))*xtemp[4];`
9. `proc8 = proc7*xtemp[11]/xtemp[3];`

The reaction terms from the ASM 1 matrix are described by the s function as “`reac 1-13`”, for the state conversion rates.

e.g

$$r_j = \xi_j v_{ij} \rho_j$$

Therefore, summing through  $j$  for each component  $i$  and multiplying the process rates with the corresponding stoichiometric coefficients for each process  $j$ .

e.g

$$r_2 = \xi_j v_{ij} \rho_j = (v_{21} + v_{22} + v_{23} \dots) \rho_j$$

Therefore

$$\text{reac2} = (-\text{proc1}-\text{proc2})/Y_H + \text{proc7}; \text{ (units gCODm}^{-3}\text{day}^{-1}\text{)}$$

The “*reac*” terms are defined:

1.  $\text{reac1} = 0;$
2.  $\text{reac2} = (-\text{proc1}-\text{proc2})/\text{Y\_H}+\text{proc7};$
3.  $\text{reac3} = 0;$
4.  $\text{reac4} = (1-\text{f\_P})*(\text{proc4}+\text{proc5})-\text{proc7};$
5.  $\text{reac5} = \text{proc1}+\text{proc2}-\text{proc4};$
6.  $\text{reac6} = \text{proc3}-\text{proc5};$
7.  $\text{reac7} = \text{f\_P}*(\text{proc4}+\text{proc5});$
8.  $\text{reac8} = -((1-\text{Y\_H})/\text{Y\_H})*\text{proc1}-((4.57-\text{Y\_A})/\text{Y\_A})*\text{proc3};$
9.  $\text{reac9} = -((1-\text{Y\_H})/(2.86*\text{Y\_H}))*\text{proc2}+\text{proc3}/\text{Y\_A};$
10.  $\text{reac10} = \text{i\_XB}*(\text{proc1}+\text{proc2})(\text{i\_XB}+(1/\text{Y\_A}))*\text{proc3}+\text{proc6};$
11.  $\text{reac11} = -\text{proc6}+\text{proc8};$
12.  $\text{reac12} = (\text{i\_XB}-\text{f\_P}*\text{i\_XP})*(\text{proc4}+\text{proc5})-\text{proc8};$
13.  $\text{reac13} = -\text{i\_XB}/14*\text{proc1}+((1-\text{Y\_H})/(14*2.86*\text{Y\_H}))-(\text{i\_XB}/14))*\text{proc2}-$   
 $((\text{i\_XB}/14)+1/(7*\text{Y\_A}))*\text{proc3}+\text{proc6}/14;$

The new state concentrations after the aeration process are then calculated by the ASM 1 model in the “*dx*” section of the C file S function.

Therefore, for the first state:

$$\text{dx}[0] = 1/\text{vol}*(\text{u}[14]*(\text{u}[0]-\text{x}[0])) + \text{reac1};$$

e.g. the model combines the reaction term with an accumulation term first dividing the accumulation term with the tank volume for compatibility with the previous “*reac*” term.

So

$$(\text{u}[14]*(\text{u}[0]-\text{x}[0]))$$

or

$$(\text{inflow}*(\text{input conc.} - \text{output conc.}))$$

expressed as a mass flowrate, then divided by the volume to give  $\text{gCODm}^{-3}\text{day}^{-1}$ . So “*dx*” is the change in concentration of a component state from which the new value is calculated by integration.

The “*dx*” terms are defined:

1.  $dx[0] = 1/vol*(u[14]*(u[0]-x[0]))+reac1;$
2.  $dx[1] = 1/vol*(u[14]*(u[1]-x[1]))+reac2;$
3.  $dx[2] = 1/vol*(u[14]*(u[2]-x[2]))+reac3;$
4.  $dx[3] = 1/vol*(u[14]*(u[3]-x[3]))+reac4;$
5.  $dx[4] = 1/vol*(u[14]*(u[4]-x[4]))+reac5;$
6.  $dx[5] = 1/vol*(u[14]*(u[5]-x[5]))+reac6;$
7.  $dx[6] = 1/vol*(u[14]*(u[6]-x[6]))+reac7;$
8.  $dx[7] = 1/vol*(u[14]*(u[7]-x[7]))+reac8+u[15]*(SO\_sat-x[7]);$
9.  $dx[8] = 1/vol*(u[14]*(u[8]-x[8]))+reac9;$
10.  $dx[9] = 1/vol*(u[14]*(u[9]-x[9]))+reac10;$
11.  $dx[10] = 1/vol*(u[14]*(u[10]-x[10]))+reac11;$
12.  $dx[11] = 1/vol*(u[14]*(u[11]-x[11]))+reac12;$
13.  $dx[12] = 1/vol*(u[14]*(u[12]-x[12]))+reac13;$
14.  $dx[13] = (u[14]-x[13])/T;$

Where the “u” terms are the state concentrations into the reactor, and the “x” terms are the new state concentrations after the bioreaction.

The concentration of dissolved oxygen in the tank, given here as:

$$dx[7] = 1/vol*(u[14]*(u[7]-x[7]))+reac8+u[15]*(SO\_sat-x[7]);$$

as discussed previously:

$$S_o = \frac{V}{Q} \cdot (S_{o_{IN}} - S_o) + kLa(S_{o_{SAT}} - S_o) + R_R$$

where:

$S_o$ =dissolved oxygen concentration (mg/l)

$V$ =tank volume ( $m^3$ )

$Q$ =volumetric flowrate ( $m^3/day$ )

$kLa$  = mass transfer coefficient ( $day^{-1}$ )

$R_R$  = reaction rate of oxygen consumption

## 2.9 Aeration System

Secondary Sludge treatment occurs at the Perth wastewater treatment plant in three aeration lanes and three final settlement tanks. The aeration tanks are made up of nine

compartments in total (three aeration lanes, each with three mechanical aerators). After the influent flow is divided in the penstocks, it remains separate until discharge into the receiving waters, with each aeration “leg” having a corresponding final settlement tank. For this reason, one aeration lane or “leg” is modelled and an assumption made that the concentration of sludge components is the same in each of the three lanes. The aerators themselves are fixed platform low speed types, each with a rated power of 12.5hp, which have been in use at the plant for some 30 years. The aerators run at full power, 24 hours a day and have been found to consume unacceptable levels of power at the plant. Suggested alternatives, in order of increasing cost, are; on-off relay control, variable speed drives on one or more of the aerators, replacement with diffused aerators and the supply of pure oxygen to the process.

### 2.9.1 Principle of Mechanical Aeration

Surface mechanical aerators achieve oxygen transfer by violent agitation of the activated sludge surface and entrainment of air by driving it into the liquid phase. The impeller used has the added advantage of dispersing air bubbles and mixing the tank contents. The agitation also maintains suspension of the sludge floc, which is central to the activated sludge process.

### 2.9.2 Aerator Performance

The performance of mechanical aerators is rated in terms of their oxygen transfer capability, which is an efficiency expressed as pounds of oxygen per horsepower-hour. Or in S.I kilograms of oxygen per kilowatt-hour.<sup>1</sup> In Metcalf and Eddy, Wastewater Engineering, Treatment Disposal and Reuse, table 10-9 gives “Typical ranges of oxygen-transfer capabilities for various types of mechanical aerators”, expressed in lb/hp.hr. Plant data on the oxygen transfer capabilities of the Perth aerators was not available on account of their age. Therefore the transfer rate of oxygen per unit energy for a “surface, low speed aerator” was used at “field” conditions. (e.g. wastewater at 15°C). 1.2lbO<sub>2</sub>/hp.h was selected from the range because it was at the lower end of the scale, assuming the aerators are relatively inefficient.

### 2.9.3 KLa and oxygen transfer in the ASM 1 model.

The concentration of dissolved oxygen in the ASM 1 model varies according to the following expression:

$$S_o = \frac{V}{Q} \cdot (S_{o_{IN}} - S_o) + kLa(S_{o_{SAT}} - S_o) + R_R$$

The second term in the relationship includes the dissolved oxygen level at saturation,  $S_{o_{SAT}}$ , taken as  $8\text{mgO}_2/\text{l}$  and  $kLa$ , the mass transfer coefficient. The  $kLa$  is a rate term here expressed in  $\text{days}^{-1}$ , where  $kLa$  is a coefficient and  $(S_{o_{SAT}} - S_o)$  is the concentration driving force according to the two film theory for gasses dissolving into the liquid phase.

### 2.9.4 Modelling of Aeration system

As discussed above, the transfer of oxygen into the activated sludge process is a function of the power supplied to the aerators. The parameter,  $kLa$ , in the ASM 1 model and thus the DO concentration in the tank can be manipulated by changing the power output of the aerators. Initially, this is used to set up the model but it can also form the basis of a closed loop control system. With suitable final control elements and DO instrumentation, manipulating the level of oxygen in the tank is possible by changing the power via a variable speed drive.

However, before this can be achieved, a subsystem must be included in the model to provide the conversion of units from power (hp) to  $kLa$  ( $\text{days}^{-1}$ ) such that it can be included in the ASM 1 model. The subsystem will also provide all the information that is required from the model, for example time in days, cost of aeration per annum, and energy use in kWhrs, to enable the straight forward comparison of alternatives to the current aeration practice.

In the below Simulink™ flow diagram the outputs are shown in red. On the right hand side, the values given for  $kLa$ , energy in kWhrs and the cost of aeration per annum are outputted back into the main activated sludge process model. From there they are sent “to workspace” where the information can be viewed or plotted in the MATLAB™ environment. The model inputs, shown in blue, can be edited from the main activated

sludge model. These are the aerator power (12.5hp) in the bottom left hand corner and the alpha factor on the left hand side. The power of the aerators is first converted to kW and then to kWhrs/day, for inclusion in the kLa/power function expressed below. The yellow function block at the top of the flow diagram contains this equation.

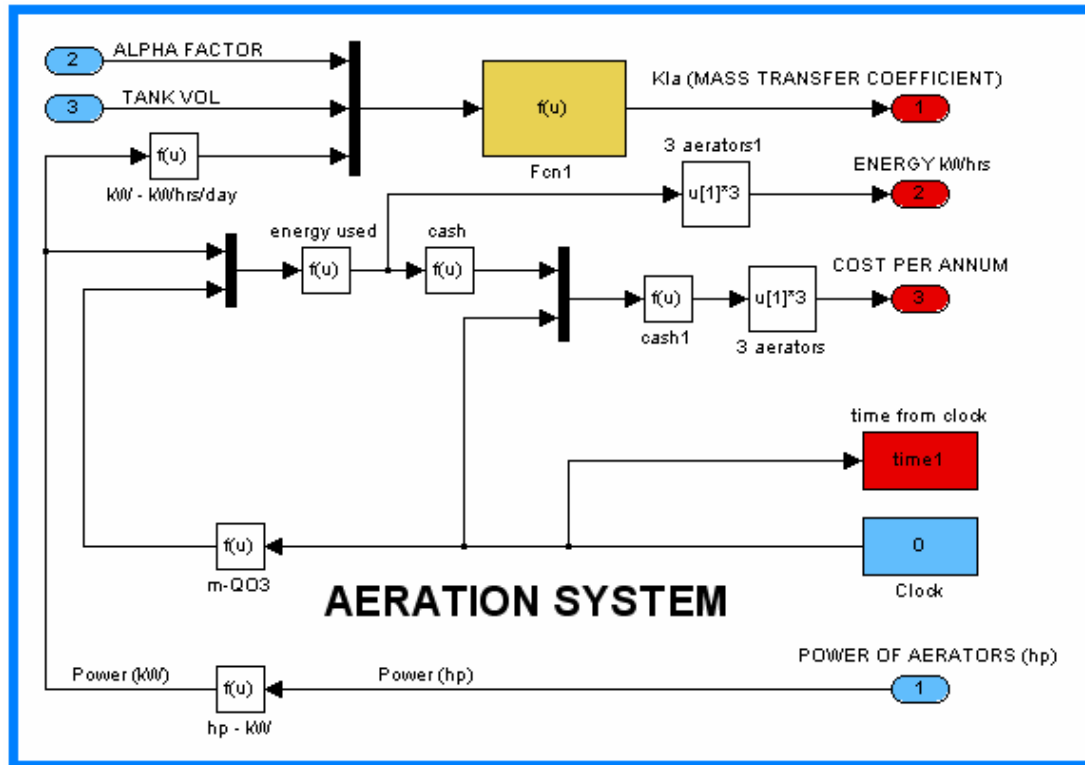


Figure 2.5: Simulink™ representation of Perth Mechanical Aeration system

The additional information given by this subsystem is the energy usage of the mechanical aerators and the corresponding annual cost given that the power usage is the same over the period of a year as it is over the modelling period. This is achieved by multiplying the power imputed into the model by the modelling time to give the energy use after a specific point in the model time. Information on the company's power tariff is then included and a factor introduced to provide annual energy cost, e.g. the cost of one kW year. The cost per kW hour was taken as 3.77pence.

The  $kLa$  for mechanical aeration is given by:

$$kLa = \alpha \cdot \frac{OP \cdot 1000}{So_{sat} \cdot V_{BB}} \cdot P \dots\dots\dots (\text{COST})$$

where:  $\alpha = 0.82$  (from Metcalf and Eddy, Wastewater Engineering, Treatment Disposal and Reuse, table 10-10 “Typical values of alpha factor for low speed surface aerators and selected wastewater types”)  
 $So_{SAT} = 8\text{mg/l}$  (dissolved oxygen saturation concentration, at 20°C)  
 $V_{BB} = \text{tank capacity} = 400.00\text{m}^3$

The value of  $O_p$  is given in Metcalf and Eddy, Wastewater Engineering, Treatment Disposal and Reuse, table 10-9 “Typical ranges of oxygen transfer capabilities for various types of mechanical aerators”. For the surface, low speed type the range is 1.2-2.4lb.O2/hp.h

Assuming the aerators have relatively low efficiency because of their age:

$$OP = 1.5 \text{ lb.O2/hp.h}$$

Converting 
$$OP = 1.5 \text{ lb.O2/hp.h} * \frac{1 \text{ kg}}{2.205 \text{ lb}} * \frac{1.3 \text{ hp}}{1 \text{ kW}}$$

$$\underline{OP = 0.912\text{kgO}_2/\text{kWh}}$$

The power supplied to the mechanical aerator, given that they are run at full power all day:

$$\text{Power} = 12.5\text{hp} * \frac{1 \text{ kW}}{1.34 \text{ hp}}$$

$$\text{Power} = 9.328 \text{ kW}$$

$$P = 9.328 \text{ kW} * 24\text{hrs}$$

$$\underline{= 223.88 \text{ kWh/day}}$$

$$kLa = \alpha \cdot \frac{OP \cdot 1000}{So_{sat} \cdot V_{BB}} \cdot P$$



$$kLa = 0.82 \cdot \frac{0.912 \cdot 1000}{8 \cdot 400.00} \cdot 223.88$$

$$\underline{kLa = 52.3 \text{ days}^{-1}}$$

Therefore the  $kLa$  (mass transfer coefficient) for each mechanical aerator is  $52.32 \text{ days}^{-1}$ .

## 2.10 Constant flow Simulations.

In the first run of the Perth WWT plant model, the Perth DWF value of  $6666.67 \text{ m}^3/\text{day}$  was used as a constant influent flow along with the recycle rate of  $1.5 \cdot \text{DWF}$  or  $10000 \text{ m}^3/\text{day}$ . Initial state concentrations were calculated according to the MATLAB file “normalization” The feed ratios present in the original “COST simulation benchmark” model were applied to the average flow value. The aeration process was simulated over a period of 7 days with a total of 1010 flow readings, taken every 10mins. This is equivalent of  $\frac{1009}{24 \cdot 6}$  days, because the telemetry data runs from midnight to the same time a week later inclusive. The sample time of the model, therefore, was  $\frac{1}{24 \cdot 6}$  days, or every 10 minutes.

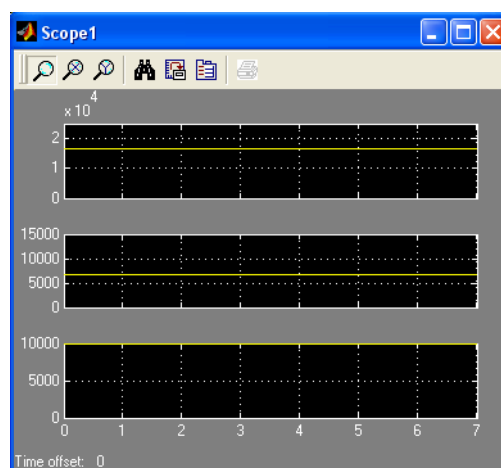


Figure 2.5:  $Q_R + Q_{in}$ ,  $Q_{in}$  and  $Q_R$

Figure 2.5 shows a Simulink scope with the flow into the reactor ( $Q_{in} + Q_R$ ) at the top, the influent flow ( $6666.67 \text{ m}^3/\text{day}$ ) and the RAS flow ( $10000 \text{ m}^3/\text{day}$ ). The graph below, (Figure 2.6) shows the dissolved oxygen concentration in the tank from

t=0days to t=7days. The blue line is the first compartment in series, the red line the second and the black line the third. This shows the dissolved oxygen concentration gradient from the start of the tank to the end. As t increases the DO concentration in each tank levels off. It can be seen that the DO concentration at the end of the tank is about 6mg/l and the DO concentration at the start of the tank is around 4mg/l, on cessation of the simulation. However, the dissolved oxygen meters are located near the tank outlet so the derived concentration in the third tank, is most representative of the Perth telemetry data.

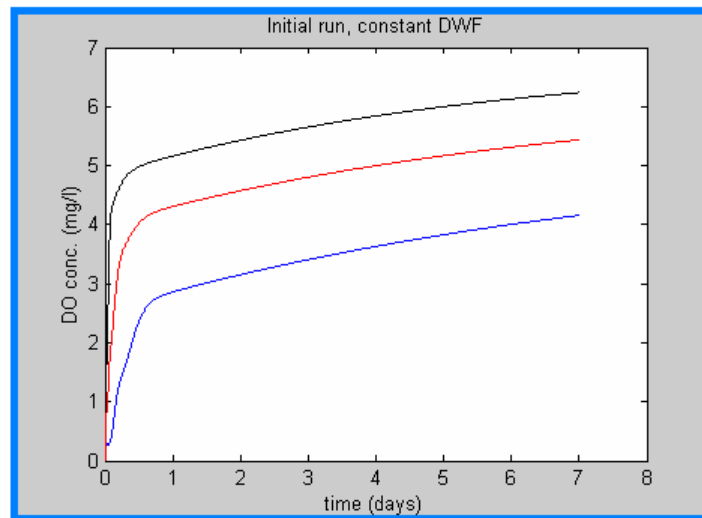


Figure 2.6: Graph of initial run, with DWF data

The DO level shows a first order curve and almost reaches a constant value of around 6mgO<sub>2</sub>/l in the final tank. The dissolved oxygen in the tank is given by:

$$So = kLa(So_{SAT} - So) - R_R$$

There is no oxygen in the inflow, and the rate at which oxygen dissolves into the tank is dependant on the value of kLa and the rate at which oxygen is removed from the tank by the microbial population, R<sub>R</sub>. The DO oxygen shows first order kinetics over the course of the simulation because as the concentration of dissolved oxygen (S<sub>o</sub>) in the tank increases, the term (S<sub>o</sub><sub>SAT</sub> - S<sub>o</sub>) decreases and the rate R<sub>R</sub> at which oxygen is removed from the tank increases as the concentration of biomass in the tank increases. The rate of oxygen transfer into the tank reaches steady state conditions where the oxygen dissolving into the tank is equal to the oxygen being removed from the tank.

When examining the DO concentration from one aeration lane in the Perth WWT plant, the average value can be seen to be around the value calculated during the simulation.

DO conc. from telemetry data= 6.09gO<sub>2</sub>/l (average over time)

Figure 2.8 shows the DO concentration from telemetry data. The real average DO data is slightly less than the value from steady state conditions in the model. This could be for a number of reasons:

- Inaccurate assumptions were made about initial state concentrations in the influent inflow.
- The DO sensors at the Perth WWT plant are situated on the wall of the tank, the model measures the state concentration of the whole tank per unit volume.
- The model may not give entirely accurate state concentrations.
- Unrealistic assumptions were made about the degree of mixing within the tank.

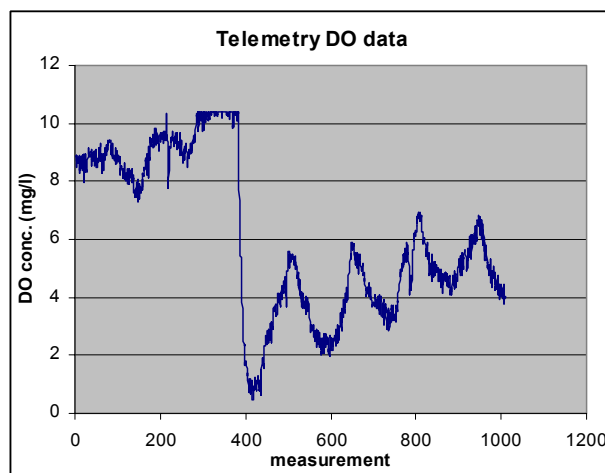


Figure 2.8– dissolved O<sub>2</sub> from telemetry data

In the second steady state simulation, an average flow from the influent telemetry data was taken, and initial state concentrations were calculated according to the MATLAB™ file: normalization. The feed ratios present in the original “COST simulation benchmark” model were again applied to the average flow value. This influent flow represents 2 times the dry weather flow in the first simulation. See figure 2.9 below.

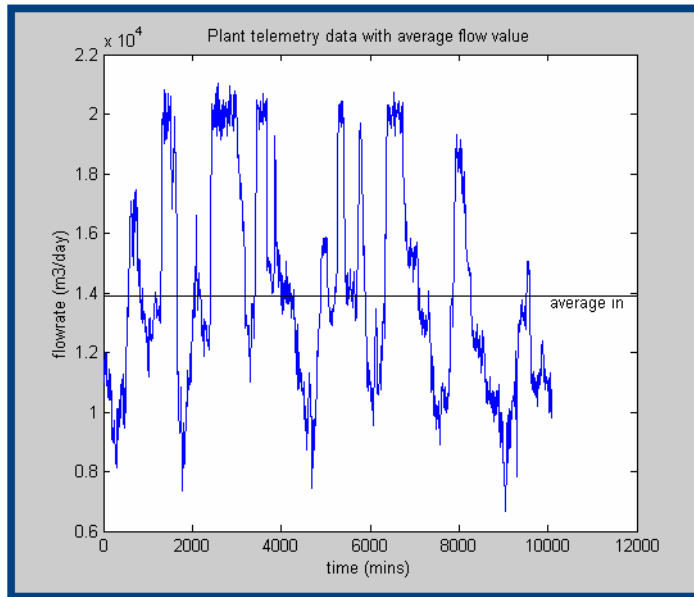


Figure 2.9– plant data with average flowrate

The DO concentration in each aeration chamber was then exported to the MATLAB™ workspace and examined by the “plot” function. Since the DO sensors at the Perth WWT plant are located on the outer wall of the tank near the outlet, the reading from the third aeration “chamber” in the model was compared to the average DO value from Perth. The flowrates as before, are:

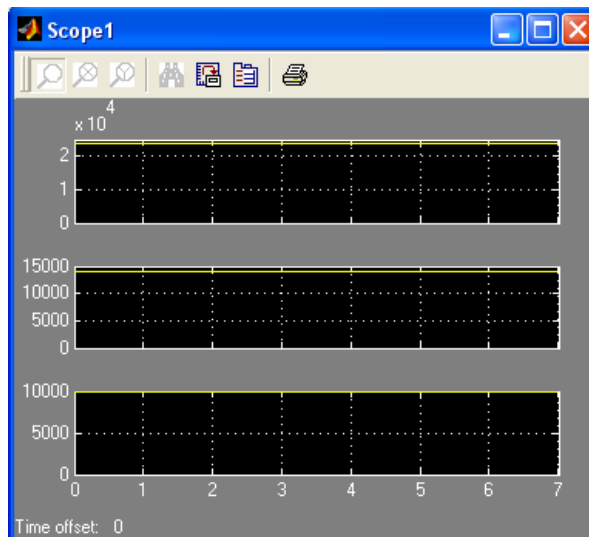


Figure 2.10: Wet weather influent

The results are shown in figure 2.11

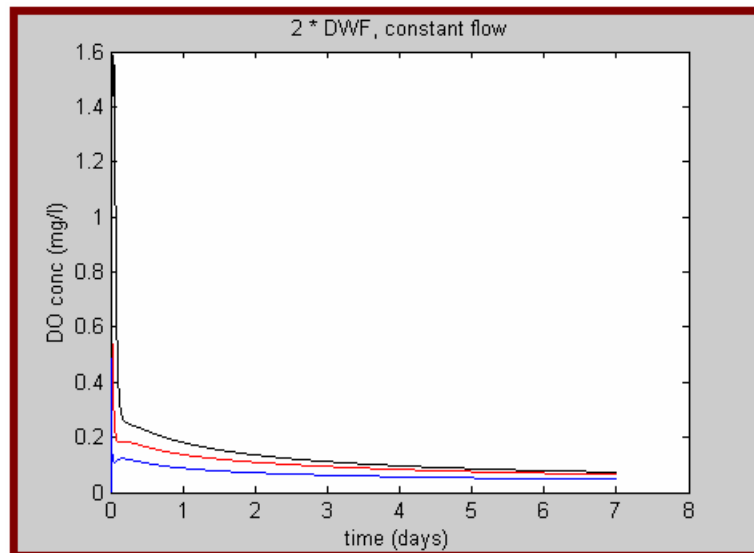


Figure 2.11:Wet weather flow results

As can be seen from figure XXX, when the flow is 2 times the dry weather flow, there is insufficient oxygen in the tank. This will be discussed in more detail later. For the rest of the report, the telemetry data will be scaled down to DWF average before commencing simulation.

### 2.11 Simulation with telemetry flow data.

When the telemetry flow data, scaled down to dry weather flow, is used as the model influent, the results show huge variations in DO concentrations over time. These variations are due to the large disturbances in the telemetry flow data. The difference between the concentration in compartment 1 and 3, suggests a DO gradient along the length of the tank. The accumulation term in the dissolved oxygen concentration equation, means that the DO concentration in one compartment is added to by subsequent compartments, and this means the DO concentration in the final compartment is higher than the other two compartments. Furthermore, the DO concentration in the first compartment is occasionally drops below 0.5mg/l. Here, there is a suggestion of oxygen starvation at the influent end of the tank. A method of tapered aeration, would overcome both these problems by supplying more oxygen to the influent end of the tank and less to the effluent end.

The large variations in DO concentration in the tank suggest that a control system could be used effectively to minimise the energy use of aerators by maintaining the dissolved oxygen concentration at a set point of around 2mg/l.

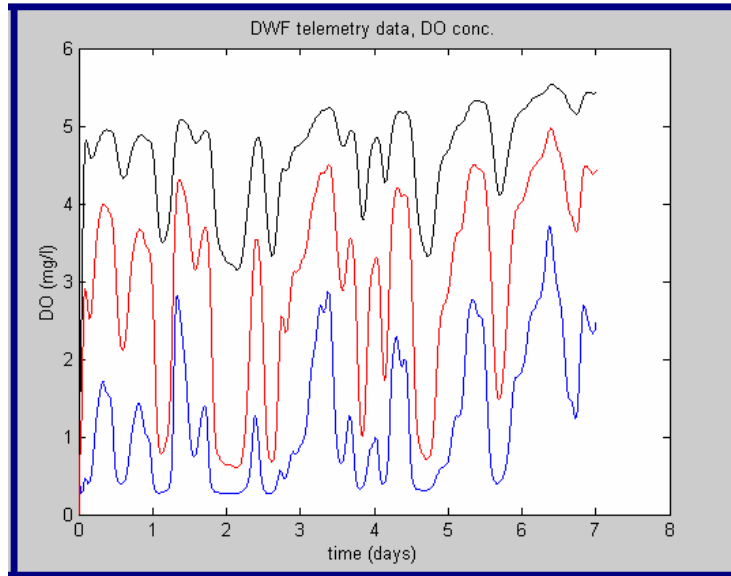


Figure 2.12: Plot of DO conc.with DRY telemetry data.

## Chapter 3: Control of the Activated Sludge Process

### 3.1 Introduction

The wastewater treatment process has not benefited from process control in the same way as the process or manufacturing industries have. Waste Water Treatment produces no marketable goods so there is limited financial incentive to introduce complicated control systems. For some, the main priority of wastewater treatment is to provide good water quality standards, thus energy saving techniques are not considered as important. (Olson + Newell 1993)

As a result, most wastewater treatment plants in Scotland have no automatic control systems at all, and as mentioned earlier, the IAWQ models which have been developed over the past 15-20 years are not in widespread use because it is still difficult to design a sensible controller based on these models. The process itself is very complex and it is not obvious how to control and optimise the plants. (Lindberg 1997). The models are also of limited value for influents other than dry weather flow. The incentive to improve the overall process, however, will ultimately be economic. Stricter penalties in the future and private ownership of treatment plants may mean the emphasis shifting to computer based control of wastewater. It is the next stage in their development.

Low cost solutions to the wastewater treatment problem are becoming more and more important. Across the industry, there is more emphasis on lowering production costs and workforces have been reduced as a result. The reduction of energy use by the implementation of better process control could contribute to the reduction of plant running costs.

At the Perth plant, however, it is clear that the installation of modern control systems, including computers and final control elements may involve considerable capital outlay. There are dissolved oxygen, MLSS and flow sensors, but many of the valves are manually operated, and pumps and motors are non-controllable. The implementation of a relay based on-off control system however could be a viable alternative to a high level control system.

### 3.2 On-Off Control

Given the large influent disturbances in wastewater treatment plants, on-off control can provide sufficiently accurate control for mechanical surface aerators relatively cheaply. However, as will be discussed, problems may arise when repeatedly switching on and off such aerators. The simple on-off controller measures the DO concentration in the tank and performs a feedback loop, turning the aerators on or off depending on the DO concentration in the tank. Tuning problems associated with PID control are not encountered with on-off or relay based control.

There are two forms of on-off control:

#### 3.2.1 A relay on-off controller:

This is a feedback controller which operates by a simple switch in a similar way to a home thermostat. It uses the controller error  $e(t)$  as a signal for the control action to begin or stop. The error at a given time  $t$  is given as the set point or desired value of DO concentration (say 2mg/l) minus the operational value of the DO concentration.

e.g.  $e(t) = sp(t) - y(t)$ . If the error is negative then the DO concentration is greater than the desired value and the control input is switched off. If the error,  $e(t) = sp(t) - y(t)$  is positive then the DO concentration is less than the desired value and the control input is switched on in order to drive the controlled output closer to the setpoint. (Katebi et al 1998).

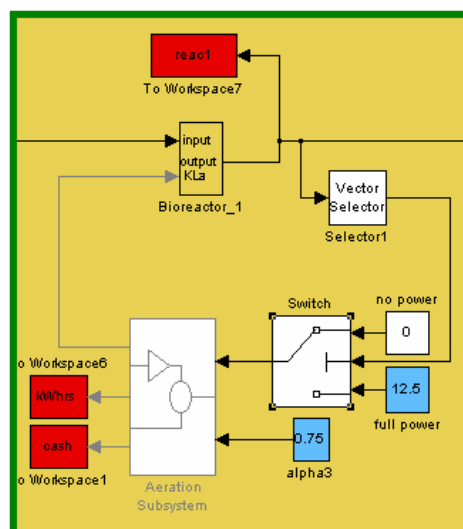


Fig 3.1: Detail of relay on-off controller model showing switch and control loop.



The algorithm is as follows:

Calculate  $e(t)=r(t)-y(t)$

If  $e(t)<0$  then control OFF

If  $e(t)\geq 0$  then control ON

Figure 3.1 above, shows a detail of the Simulink flow diagram. The vector selector function selects the desired state variable from the tank, in this case the dissolved oxygen concentration, for inclusion as the measured variable in the on-off controller. The output of the switch function, i.e. the power input to the aeration subsystem block, depends on the value of the measured variable. If it is above the setpoint, as selected by selecting the switch block, the input to the aeration subsystem will be 12.5hp, the rated power of the surface aerators at the plant. If it is below the setpoint, the input to the aeration subsystem will be 0hp, thus indicating the cessation of the control signal and the turning off of the corresponding aerator. The switch system was included for all three aerators in the lane independently. However, this style of control system is unstable, and delays or rate limiters have to be included to stop the control response oscillating rapidly. The pitch of these oscillations depends on the speed of response of the process to the controller's on-off action. (Olsson et al 1993). When the air is turned off, the rate at which the DO falls is related to the oxygen uptake rate (OUR), or the reaction rate ( $R_R$ ) of the biomass. This term is large compared to the accumulation term in the original DO mass balance, so the DO level falls rapidly. The nature of this response causes rapid cycling and would cause *chattering* of the controller and stress to the mechanical aerator itself. Due to the nature of the control system, the computer was unable to carry out the simulation.

### 3.2.2 Threshold On-Off controller of all three Aerators.

In threshold on-off control there is a range of values, e.g.  $r(t)+d$ , of measured variable where the controller does not change. If the actual output  $y(t)$  exceeds  $r(t) + d$ , then the control is switched off. The control remains off until the actual output  $y(t)$  falls below  $r(t) -d$ , where it is switched on. If the actual output  $y(t)$  is below  $r(t) -d$ , then the control is switched on, until the actual output  $y(t)$  exceeds  $r(t) +d$ .

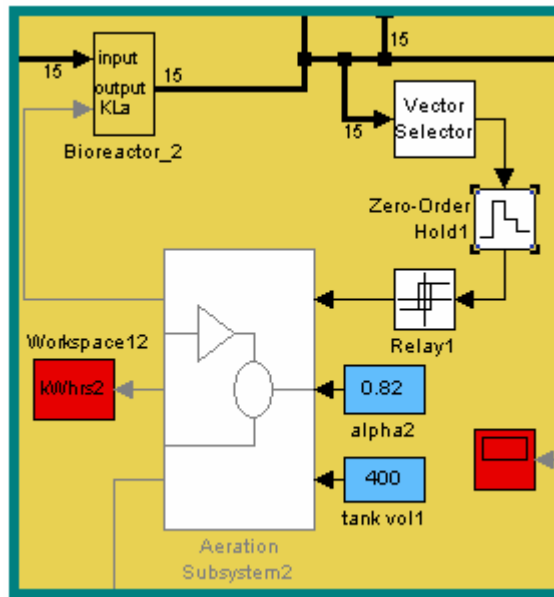


Figure 3.2: DO controller with threshold on-off control

In the below diagram, the limit cycling is greatly reduced by adding a relay with threshold limits. The parameters were as follows:

Switch on point: 3.5mg(DO)/l

Switch off point: 2.5mg(DO)/l

Output when ON: 0hp

Output when OFF: 12.5hp

The threshold on-off controller was applied to all three aerators in the aeration lane, the Simulink flow diagram with the threshold controller is shown in figure 3.2.

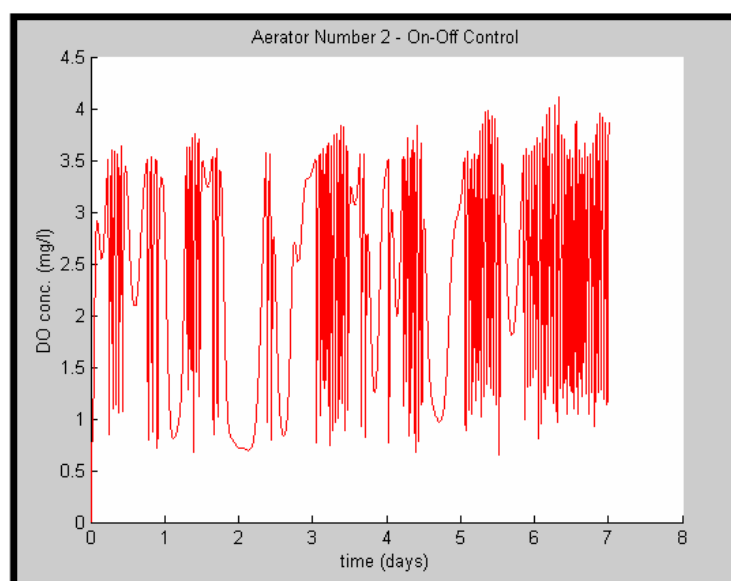


Figure 3.3 – Controlled response of an On-Off threshold controller, threshold values 3.3-2.5mg/l

A zero order hold block was added before the relay to limit the sampling rate of the control system to every 30 mins. This means that theoretically, the control system is capable of shutting the aerator off or turning it on every half an hour depending on the influent disturbances. Such a high rate of switching could add considerable stress to the aerators but through experimentation with different rates it was discovered that when the switching rate was lowered, the on-off mechanism did not exercise sufficient control over the process. With a reasonably large range of threshold values however, the switching would not be as frequent as every half hour, and the control system might prevent excessively high dissolved oxygen levels in the tank, although the energy saving would not be as great. The controller response for the second aerator is shown in fig 3.3 (above).

From the above discussion, the disadvantages of this kind of control are clear. Smooth control is impossible to achieve, and stress to apparatus is highly likely. The dynamic response in the process is too high to make On-Off control viable. Additionally, on-off control of all three aerators, from the simulation results generated, is probably the best use of this control system. Each aerator is turned on and off according to the DO concentration in each aeration compartment, so from the simulated data, when one aerator is turned off, the concentration in the next compartment falls, and the subsequent aerator is turned on. Similarly if the concentration falls and the first aerator is turned on, then the DO level in the next compartment is reduced below the threshold level and the corresponding aerator is turned off. The result is in phase switching, e.g. they are all switching either on or off at the same time. In practise, of course, there is a greater degree of mixing in the tank as the compartments in the model are assumed separate. However, with increased flows and correspondingly reduced residence times, this could become possible. From figure 3.3 the DO concentration is seen to fall below a level at which oxygen starvation occurs ( $<1\text{mg/l}$ ). The energy savings and associated cost with the implementation of an On-Off control system are discussed in chapter 4.

## 3.2 PID Control of the Activated Sludge Process

PID control can be used to regulate the dissolved oxygen concentration in the process by calculating the difference between the operational DO value (measured variable) and the desired DO value (set point). This difference or “error” is minimised by tuning a PID controller and the magnitude or “gain”, of the proportional, integral and derivative terms. In the activated sludge process model, the power supplied to the mechanical aerators, via a variable speed drive, or the flowrate of air delivered to the tank varies according to this error. A brief description of each term is given below.

### 3.2.1 Proportional Control

A proportional control response produces an output change in proportion to a varying input. Here, there is a linear relationship between the input and the output. If an offset exists between the measured variable and the setpoint, the proportional controller reduces the error, the speed of response depending on the value of the gain,  $K$ , thus:

$$U_c(s) = K_p \cdot e(s)$$

Where

$U_c(s)$  is the controller response

$K_p$  is the proportional gain

$e(s)$  is the error, e.g. measured variable – set point.

A setpoint, throttling range and action typically define this proportional gain in this relationship. In a proportional control response, there is a unique value of the measured variable that corresponds to full travel of the final control element (actuator or control valve) and a unique value that corresponds to zero travel on the controlled device. The change in the measured variable that causes the controlled device to move from fully closed to fully open is called the throttling range. It is within this range that the control loop will work, assuming that the system has the capacity to compensate for the disturbance.

The action dictates the gain or magnitude of the control response. In a direct acting proportional control response, the output will rise with an increase in the measured variable. In a reverse acting response, the output will decrease as the measure variable increases. Therefore increasing  $K_p$  speeds up the system response and decreases any

existing steady state offset. However, excessively large values of can saturate actuators and allowances must be made in tuning for the dynamic response, hysteresis and deadband of final control elements.

### 3.2.2 Proportional plus Integral (PI) Control

The integral part of the PID algorithm is always used with proportional control. The control now involves the measurement of the “error” or offset over time. The error is integrated and a further adjustment is made to the output signal from the proportional part of this model. This type of control response will use the control loop to reduce the offset to zero operating in a narrow band close to the setpoint. It will not operate over the entire throttling range. Integral control when added to proportional control will reduce steady state offsets. The integral term is given as:

$$U_I(s) = K_I \int^t e(\tau) d\tau$$

Where  $U_I(s)$  is the integral response  
 $K_I$  is the integral gain  
 $e(\tau)$  is the error.

PI control loops do not perform well when setpoints are dynamic or in processes where sudden load changes occur.

### 3.2.3 Proportional, Integral and Derivative Control (PID)

PID control adds a predictive element to the control response. The derivative control term provides a controller output that is proportional to the rate of change of the difference between the actual value of the parameter (temperature) and the set point. Here, in addition to the proportional and integral calculation, the derivative or slope of the control response will be computed. This term has the effect of dampening the overshooting of a control response although it has no effect on the steady state offset.

**Given by:**

$$U_D(s) = K_D \cdot de/dt$$

Where  $U_D(s)$  is the controller response

$K_D$  is the derivative gain

$de/dt$  is the rate of change of the error.

### Implementation of PI control

For the mechanical aeration system, a PI control system was implemented in much the same way as the On/Off control system by selecting the dissolved oxygen state from each reactor and using it as the measured variable for the controller. A second subsystem was created for the PI controller with two inputs, the DO set point, and the measured DO level from the ASM model. The set point was chosen as 2mg/l and the PI block was laid out as shown in figures 3.4 and 3.5:

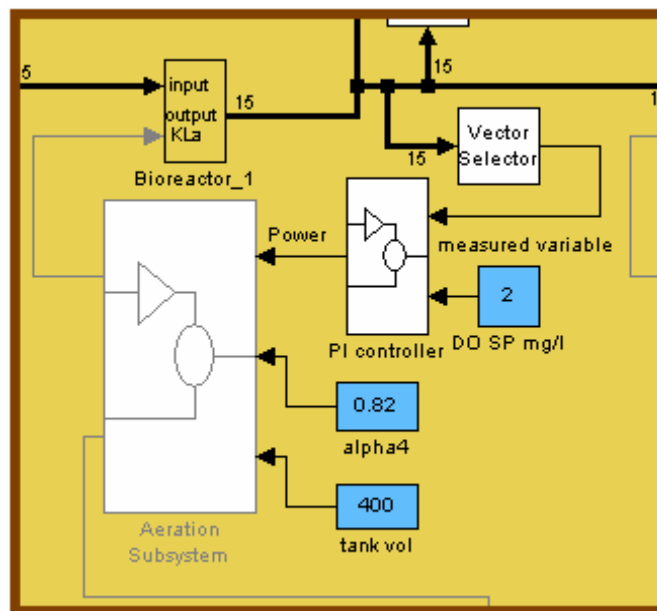


Figure 3.4: Simulink diagram of PI controller

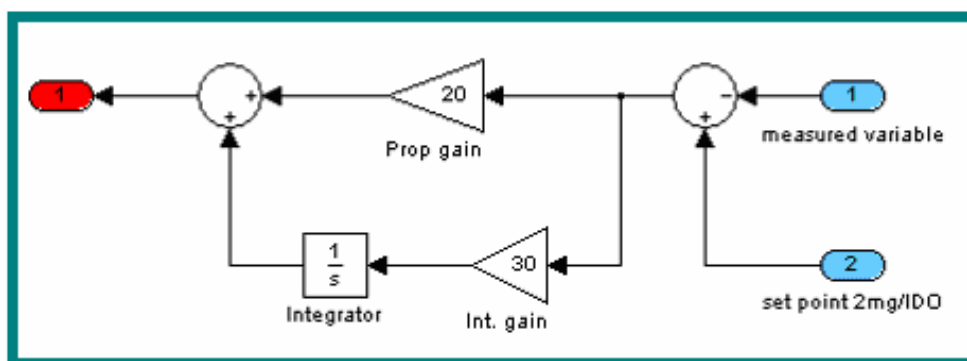


Figure3.5: PI controller showing int. and prop.gains

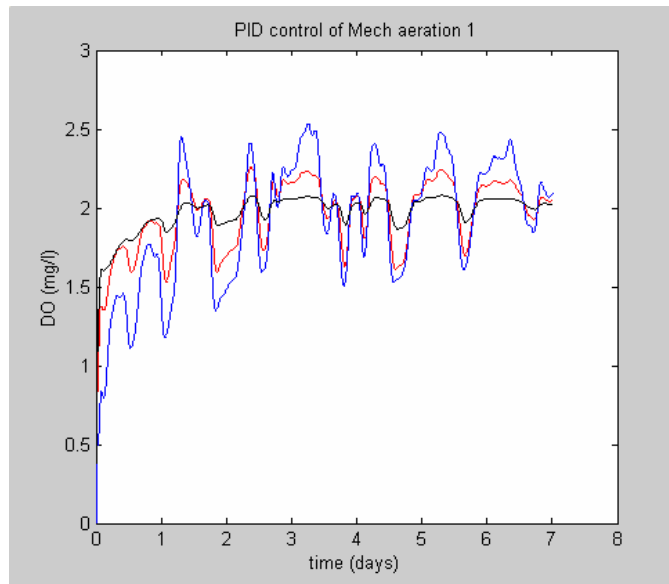


Figure 3.6: Initial controlled DO levels

As can be seen from the plot of the controlled DO concentration, the controller has a greater effect on the level in the final tank. This is because the controller gains were equal, e.g. proportional gain,  $K_p=10$  and integral gain,  $K_i=20$ , for all three aerators. For the second attempt, the gains were increased  $K_p=20$ ,  $K_i=30$  for the first aerator,  $K_p=10$ ,  $K_i=20$  for the second and  $K_p=5$ ,  $K_i=10$  for the third. The result is shown in fig xxx below. It shows the oxygen levels in each aeration compartment becoming more similar and the dissolved oxygen gradient across the length of the tank lessening.

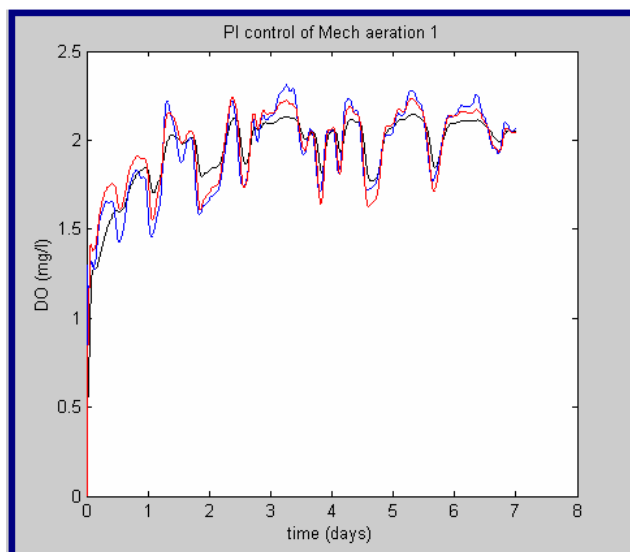


Figure 3.7: Controlled DO levels (second simulation)

For the third tuning attempt, the gains were increased to  $K_p=35$ ,  $K_i=45$  for the first aerator, to  $K_p=20$ ,  $K_i=30$  for the second and the third was kept at  $K_p=5$ ,  $K_i=10$ .

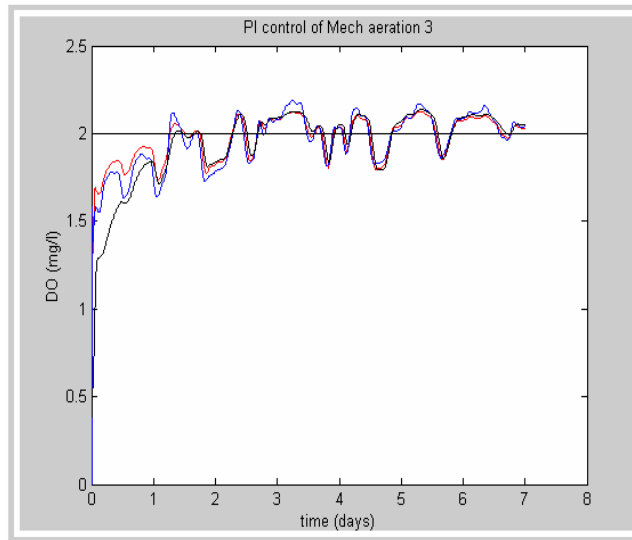


Figure 3.8: Third tuning attempt of PI controller for mechanical aeration.

The result is shown in fig 3.8. It shows dissolved oxygen levels in each aeration compartment almost identical, corresponding with the reduction of the dissolved oxygen gradient across the tank.

As can be seen from the blue plot, the dissolved oxygen concentration in the first aeration compartment tends towards the set point and the intermittent low oxygen levels characteristic of the first aeration compartment have been eliminated. This means that the aerators have to be capable of delivering more than 12.5hp to achieve this method of control. (see figure 3.9)

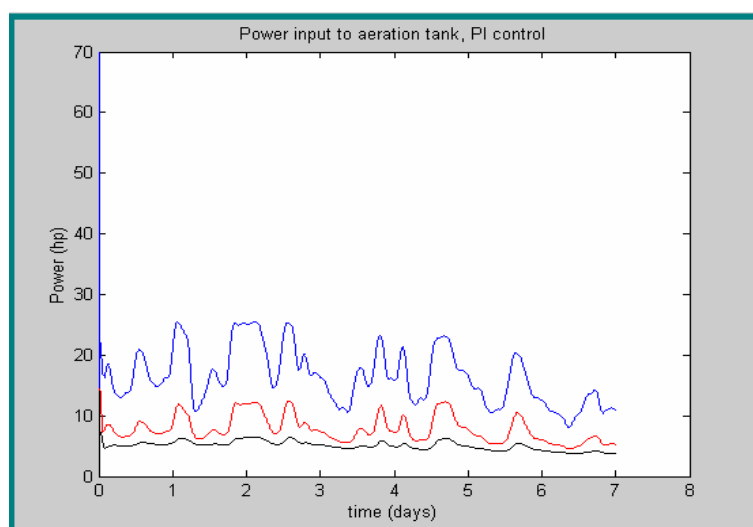


Figure 3.9: Power supplied to aerators by PI controller



To give a more realistic impression of the installation of variable speed drives at the WWT plant, a limit must be placed on the power input in the model. This can be achieved by placing a switch in the aeration subsystem as shown.

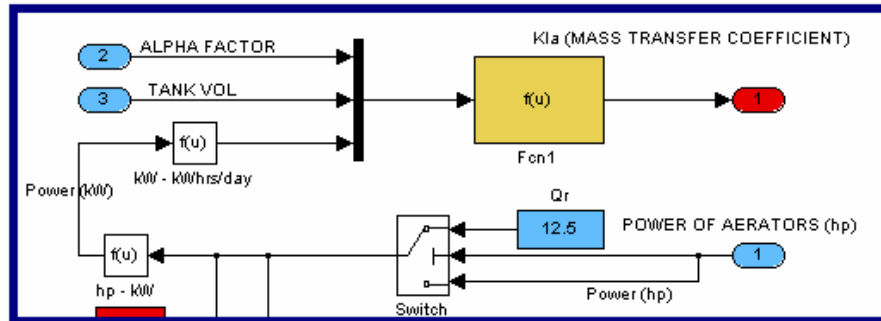


Figure 3.10: Limitation of Aerator Power

The power supplied to the aerators here is shown in figure 3.11, with the power limit set at 12.5hp.

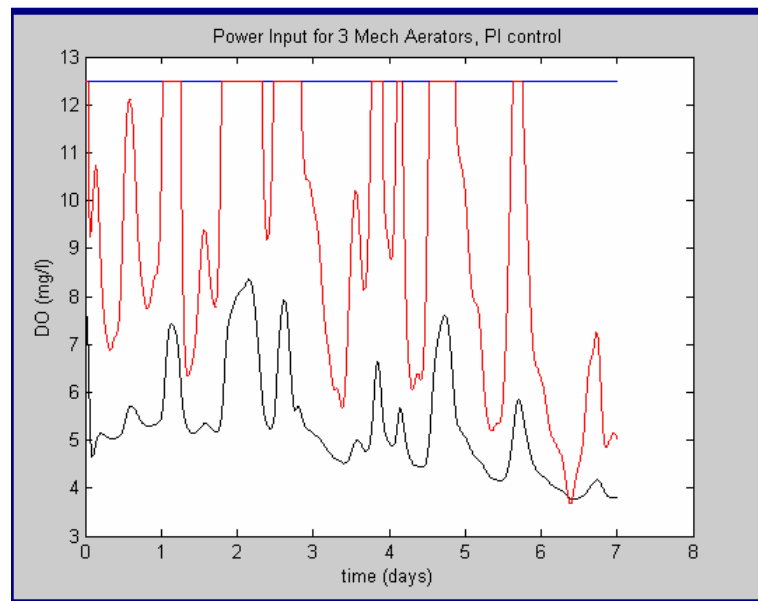


Figure 3.11: Limitation of Aerator Power

### 3.3 Diffused Aeration

Diffused aeration is one of the two basic methods of aerating wastewater (Metcalf and Eddy) whereby oxygen is pumped by blowers, at a relatively low pressure, to a number of orifices on the floor of the aeration tank where it is allowed to bubble up through the liquor. The energy use, compared to mechanical aeration is lower because in effect the air is allowed to diffuse directly into the liquid phase without the violent agitation of the sludge associated with mechanical aeration. Mechanical aeration relies on the promotion of solution of air from the atmosphere while diffused aeration introduces fine bubbles of air into the mixture, thus maximising the air transfer surface area. A diffused air system comprises submerged diffusers, and the header pipes, air mains and appurtenances through which the air is passed. The purpose of this section is to size a possible diffused aeration system and compare the oxygen transfer characteristics and energy use with the present mechanical aeration system.

#### 3.3.1 Diffused Aeration Oxygen Transfer Characteristics

The  $kLa$  for diffused aeration is a function of the flowrate of air into the tank from the submerged diffusers. Given by the COST symposium:

$$kLa_{diffused} = \alpha \cdot \frac{R_{air} \cdot h_{air}}{So_{sat} \cdot V_{BB}} \cdot Q_{air}$$

where:

$\alpha$  = alpha factor

$So_{SAT}$  = dissolved oxygen saturation concentration (taken as 8mg/l, at 20°C)

$V_{BB}$  = Volume of aeration chamber, a third of full tank volume. (400m<sup>3</sup>)

$Q_{air}$  = Flowrate of air (m<sup>3</sup>/day)

$R_{air}$  = O<sub>2</sub> flow per volume and immersion depth in clean water at  $S_0=0$  and a specified temperature (T=20C) Given in COST benchmark manual as 16g/(m<sup>3</sup>/m).

$h_{air}$  = depth of submersion of diffusers, e.g. level in tank. (m)

Where

$$h_{air} = \frac{V_{BB}}{l^2}$$

where

$l$  = length of side of tank compartment.

$$h_{air} = 400/10.7^2 = \underline{3.43m}$$

To compare diffused and mechanical aeration in order to give an estimate of the difference in energy use, the oxygen requirement from the mechanical aeration can be used in the calculation for the  $kLa$  of the diffused aerator. The assumption here is that for every 12.5hp mechanical aerator in the first calculation there would be an equivalent blower supplying air by diffused aeration.

In Biological Wastewater treatment (Grady Jr et al) page 404, the  $kLa$ /power equation for mechanical aeration can be rearranged to give the oxygen requirement satisfied by a mechanical aerator of power “P”, with an oxygen production efficiency,  $O_p$ . (kgO<sub>2</sub>/kWh).

Thus

$$RO_{mechanical} = P * O_p.$$

where

$$OP_{mechanical} = 0.912\text{kgO}_2/\text{kWh}$$

and

$$P_{mechanical} = 9.328 \text{ kW}$$

so

$$RO_{mechanical} = 9.328 \text{ kW} * 0.912\text{kgO}_2/\text{kWh} \\ = \underline{8.507 \text{ kgO}_2/\text{hr}}$$

In Biological Wastewater treatment (Grady Jr et al) page 4044, equation 10.21 gives the volumetric air flow rate in m<sup>3</sup>/min for diffused aeration, thus using the same oxygen requirement calculated previously for mechanical aeration:

$$Q = \frac{6.0 * RO}{\eta_Q}$$

where

$Q$  = volumetric flowrate (m<sup>3</sup>/min)

$$RO = \underline{8.507 \text{ kgO}_2/\text{hr}}$$

And

$\eta_Q$  = the field oxygen transfer efficiency expressed as the percent of the oxygen in the air that is transferred

into the liquid. Given as 6 – 15% in Biological Wastewater treatment (Grady Jr et al).

Assuming the aerators to have a value of  $\eta_Q = 8\%$

$$Q = \frac{6.0 * RO}{\eta_Q} = \frac{6.0 * 8.507}{8} = \underline{6.38 \text{ m}^3/\text{min of air}}$$

or

$$Q = 6.38 \text{ m}^3/\text{min} * 60 * 24 \\ = \underline{9187.56 \text{ m}^3/\text{day}}$$

Hence the diffused aerators produce an air flowrate of 9187.56 m<sup>3</sup>/day.

Therefore the equivalent Power for Diffused Aerators, given the same oxygen requirement, is:

$$kLa_{diffused} = \alpha \cdot \frac{R_{air} \cdot h_{air}}{So_{sat} \cdot V_{BB}} \cdot Q_{air}$$

$$kLa_{diffused} = 0.5 \cdot \frac{16 * 3.43}{8 * 400} \cdot 9187.56$$

$$\underline{kLa_{diffused} = 78.78 \text{ days}^{-1}}$$

Thus the oxygen transfer capability of diffused aerators is greater than that of mechanical aerators for the same oxygen requirement. However, how does the power consumption of diffused aeration compare to mechanical aeration.

The power requirement for the adiabatic compression of a blower for the replacement diffused aeration system is given in Wastewater Engineering, Metcalf and Eddy p565 by:

$$P_w = \frac{wRT}{29.7n.e} \left[ \left( \frac{P_2}{P_1} \right)^{0.283} - 1 \right]$$

where

$P_w$  = power requirement of each blower (kW)

$w$  = mass flow rate of air (kg/sec)

$R$  = gas constant for air (8.314kJ/kmol.K)

$T$  = absolute inlet temperature (K)

$P_1$  = absolute inlet pressure, (atm)

$P_2$  = absolute outlet pressure (atm)

$n = (k-1)/k = 0.283$  for air (dimensionless)

29.7 = constant for

$e$  = efficiency, assumed to be 0.8, or 80% efficient

From Metcalf and Eddy, the inlet pressure can be taken as atmospheric, and “rated discharge pressures normally range from 7-9psi”. If the assumed  $P_2$  is, the difference in pressure across the blower is:

$$P_2 = 14.7\text{lb/in}_2 + 9\text{lb/in}_2 = 23.7 \text{ lb/in}_2.$$

$$P_1 = 14.7\text{lb/in}_2 \text{ (atmospheric pressure)}$$

So  $(P_2/P_1) = 1.61$

And  $w = 9187.56\text{m}^3/\text{day} * 1.2\text{kg/m}^3 * \frac{1(\text{day})}{3600 * 24(\text{sec.s})}$

$$w = \underline{0.128\text{kg/sec}}$$

$$P_w = \frac{0.128 * 8.314 * 293}{29.7 * 0.283 * 0.8} [(1.6)^{0.283} - 1]$$

$$P_w = 46.37 * 0.142$$

$$P_w = \underline{6.597\text{kW} \text{ or } 8.840\text{hp}}$$

Therefore the power requirement of the blower for diffused aeration is 8.8hp compared to 12.5hp for mechanical aeration. However, line losses must be taken into consideration to consider the overall power requirement. See Appendix 7. Metcalf and Eddy states that pipe bends, and exit losses are small compared to friction losses over the length of pipe that cover the tank floor. The head loss occurring in the pipes of the aeration system is found to be very small. This power needed to overcome the head loss in the piping and pipe exit and entrances, is also very small, and does not affect the energy intensity of the process of diffused aeration to any measurable degree.

To give a real comparison of the two modes of aeration, however, the power requirement for a diffused system should be calculated which gives exactly the same oxygen profile in the tank. As we have already found out, the diffused aeration system of equivalent oxygen requirement uses less energy and actually delivers more oxygen to the process. Now we will calculate the power of diffused aerator that gives the same oxygen transfer (kLa) as the mechanical aerators at the Perth WWT plant.

Rearranging mechanical aeration kLa expression:

$$Q_{air} = \frac{kLa_{mech} * SO_{SAT} * V_{BB}}{\alpha_{diff} * R_{air} * h_{air}}$$

$$Q_{air} = \frac{52.32 * 8 * 400}{0.5 * 16 * 3.43}$$

$$Q_{air} = \underline{6101.55m^3/day}$$

So

$$P_w = \frac{wRT}{29.7n.e} \left[ \left( \frac{P_2}{P_1} \right)^{0.283} - 1 \right]$$

$$P_w = \frac{0.095 * 8.314 * 293}{29.7 * 0.283 * 0.8} \left[ (1.6)^{0.283} - 1 \right]$$

$$P_w = 34.28 * 0.14$$

$$P_w = \underline{4.800kW \text{ or } 6.431hp}$$

So a diffused aeration system with equivalent oxygen transfer properties requires 6.431hp compared to 12.5hp with the current mechanical aerators, about half the current energy consumption.

This energy saving could be further reduced with the implementation of a PID based control system.

### 3.3.2. Diffused Aeration PID control

In order to reduce the cost of the diffused aeration system further a PI controller was included in by using the same method as before, for the mechanical aeration system. Since the oxygen transfer for diffused aeration systems is a function of the air flow rate supplied by the diffusers, this time the air flow rate to the tank was adjusted in order to bring about changes in the tank dissolved oxygen level. As before the set point was set at 2mg/l and the aeration subsystem for diffused aeration is shown below in figure 3.12.

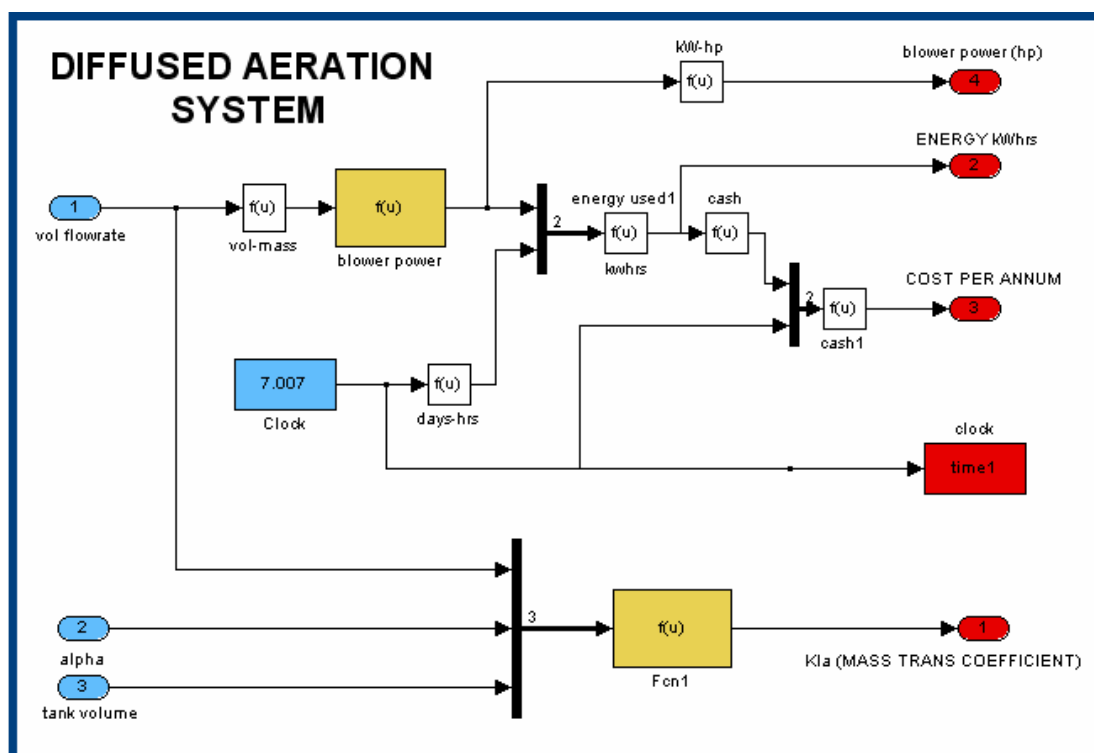


Figure 3.12 – Diffused aeration system Simulink™ flow diagram

A detail of the Simulink flow diagram for the diffused aeration with PI control is shown in figure 3.13. The PID gains were tuned in the same way as before, this time however, the gain values were considerable larger because the output from the PID block is the air flow rate supplied from the diffusers in m<sup>3</sup>/day and previously the PID output was the power in hp. The simulation results can be seen in figure 3.14 when the PID gains are set at:

Controller 1:  $K_p=10000$ ,  $K_i=10000$

Controller 2:  $K_p=5000$ ,  $K_i=8000$

Controller 3:  $K_p=2000$ ,  $K_i=5000$

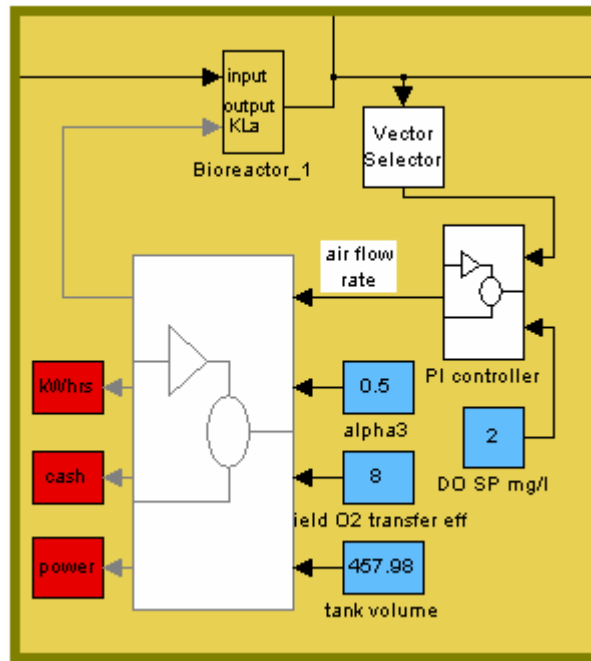


Figure 3.13: Detail of Simulink flow diagram for PI control of diffused aeration

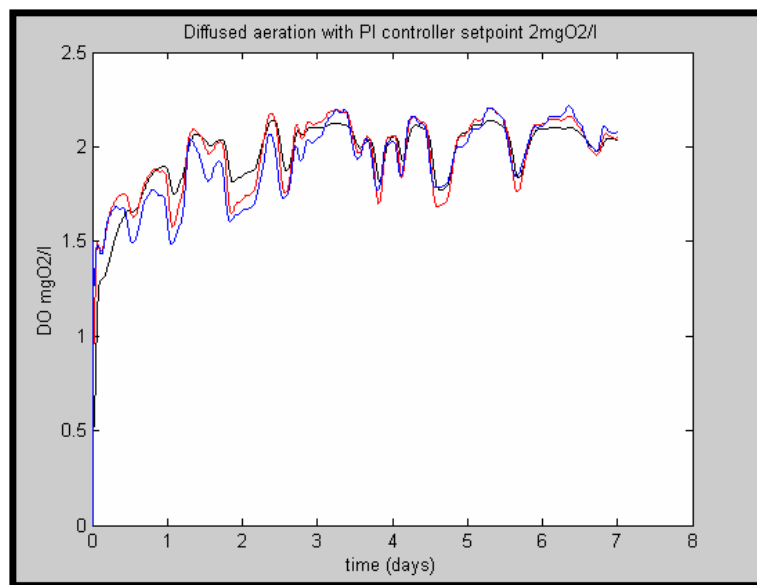


Figure 3.14: DO concentration in three aeration compartments.

In figure 3.15, the power supply to each of the three blowers is shown, the average power input to the blowers is calculated using the Simulink “mean” function to be 4.19hp for each blower. The power input is even less than previously calculated for the diffused aerator with the equivalent oxygen transfer capability because the DO concentration is lowered by the PID controller. Because of the accumulation of dissolved oxygen from one aeration compartment to the next in the model, or the real life DO concentration gradient across the tank, aerators two and three use a much



reduced power input than the first aerator. This reduction may not be as significant in reality however, again because of the initial assumptions about mixing between aeration compartments in the model.

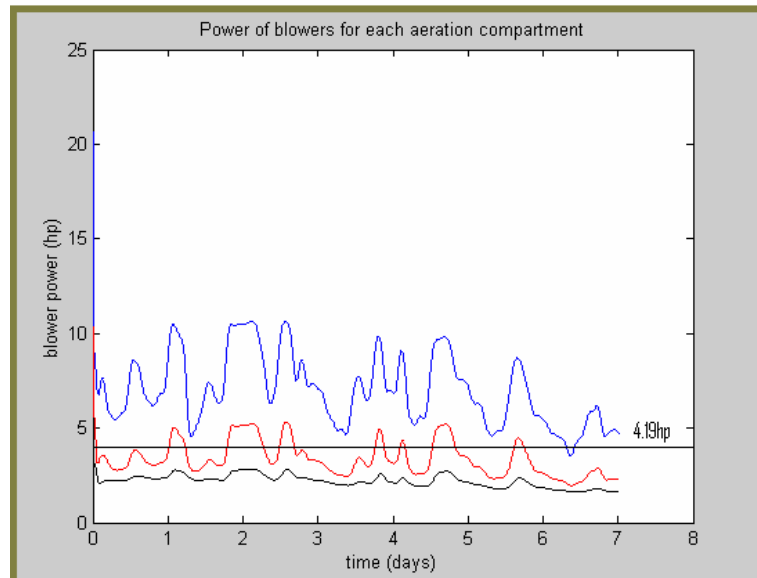


Figure 3.15: Power supply to three diffused aeration blowers

## Chapter 4 – Discussion and Conclusion

### 4.1 Cost of each mode of aeration

The following will present the energy associated cost of one aeration lane, for each of the modes of aeration and control techniques.

#### 4.1.1 Mechanical no control

The present mechanical aeration system uses energy constantly over the course of the year assuming they draw 12.5hp all the time.

Since  $1 \text{ year} = 24 * 365 = 8760 \text{ hours}$

and  $12.5 \text{ hp} = (12.5 / 1.34) \text{ kW} = 9.328 \text{ kW}$

They consume

$$E = 9.328 * 8760 = 81716.42 \text{ kWhrs in one year.}$$

We know the tariff is 3.77p/kWhr

So the electricity cost is 3.77p/kWhr

$$\text{Cost} = 0.0377 \text{ £/kWhr} * 81716.42 \text{ kWhrs/year}$$

$$\text{Cost} = 0.0377 \text{ £/kWhr} * 81716.42 \text{ kWhrs/year}$$

$$\text{Cost} = \text{£}3080.71/\text{year}$$

With 3 aerators per tank:

$$\text{Cost} = \text{£}9242.13/\text{year}$$

#### 4.1.2 Mechanical On-Off control of all three aerators.

In the case of the on-off control model, the cost of aeration is a function of the time that the aerators are kept on, since the power input is constant. In the simulation, the annual cost output from each aeration subsystem is added and an average value is taken in the Simulink block “mean” (shown in the bottom left hand corner of figure 4.1). The value is calculated over time and sent to the MATLAB workspace. In this control system the annual cost was £8014.73 representing a saving of £1227.40 a year, according to the model.



Figure 3.9 shows the power of all three mechanical aerators with a PI controller, and the power of the first aerator is always above its rated power of 12.5hp. However, with the PI controller in place the projected annual cost against simulation time can be seen in figure 4.2. With the PI controller and power limitation the projected annual cost of mechanical aeration is shown in figure 4.3.

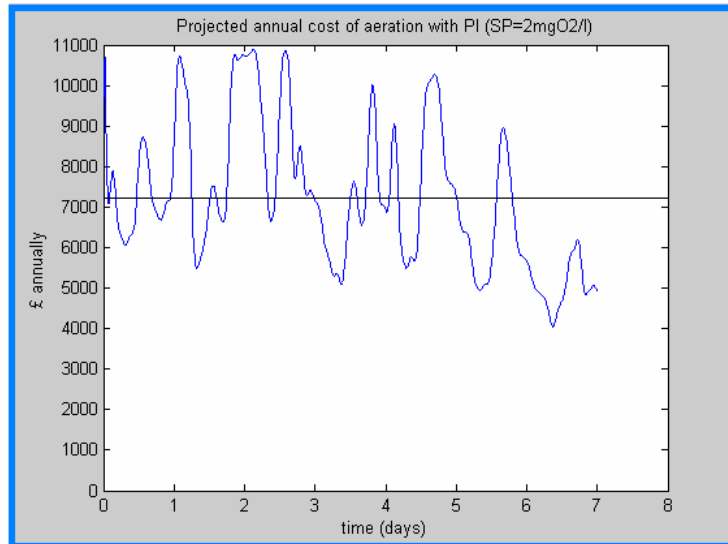


Figure 4.2 – Projected annual cost of mechanical aeration with PI controller and no power limitation.

The projected yearly cost of mechanical aeration with PID control = £7230.52

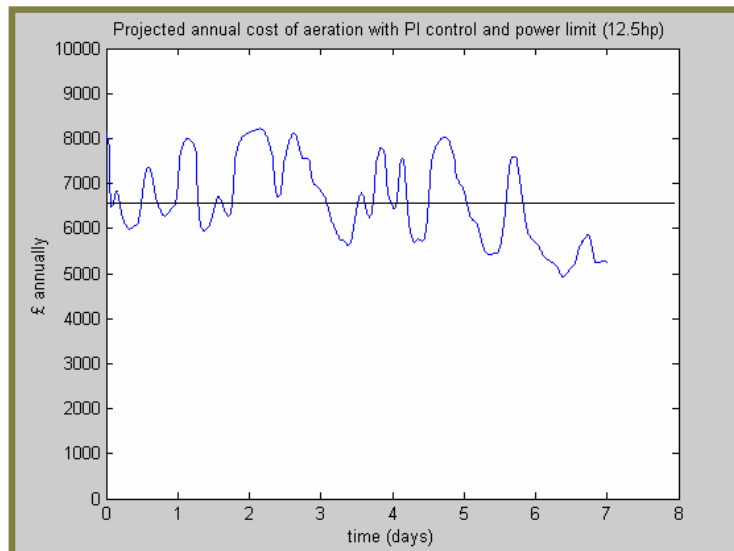


Figure 4.3 – Projected annual cost of mechanical aeration with PI controller and power limitation.

Projected yearly cost of mech aeration with PID control (max power 12.5) = £6578.66

#### 4.1.6 Diffused Aeration.

By replacing the existing mechanical aeration system with a diffused aeration system, there should be a significant energy saving. The alpha factor of diffused aeration is smaller than the value for mechanical aeration (0.5 compared to 0.82, Metcalf and Eddy). However, the oxygen transfer rate, given by the kLa coefficient, is greater for the same oxygen requirement as described in chapter 3. This means that more oxygen transfers into the sludge liquor and less energy is required for the process.

The diffused aeration system in place may not be entirely realistic, since one blower could be used to supply air to the whole lane or even the entire process. However, by using the same oxygen requirement for diffused aeration as mechanical the two systems can be compared and the cost of aeration for this system is £6536.03 a year according to the model.

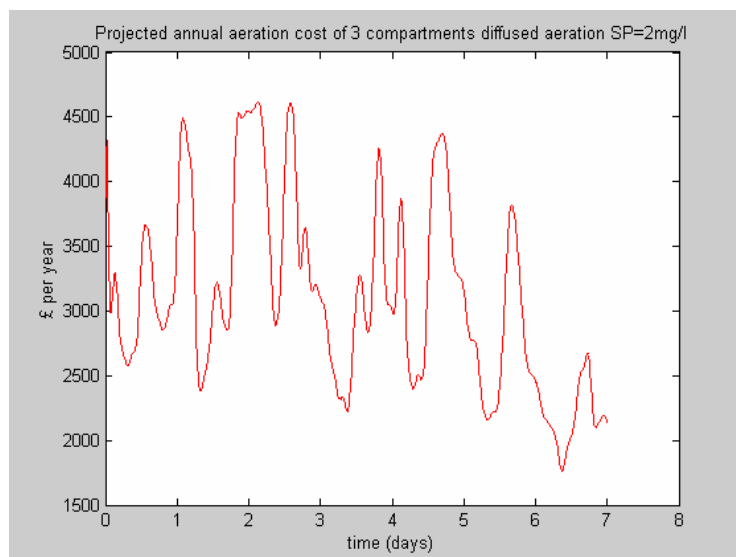


Figure 4.4– Diffused Aeration Cost with PID

The power use is further reduced when we consider the increased oxygen transfer with a diffused system due to the fine bubbles and large surface area between the liquid and gaseous phase in the tank. When the kLa for the mechanical system is substituted into the rearranged kLa/flowrate expression for diffused aeration, it yields a flowrate which results in a further decrease in power usage by the blowers and a lower annual energy cost. This system has an annual energy cost of £4249.73 according to the model.

However, the above system gives the same DO levels as the mechanical system so with the implementation of a PID controller with the diffused aeration system the annual energy cost is further reduced to £3097.96 according to the model, around a third of the original annual energy cost. (Figure 4.4)

The power input to the blowers was calculated to be negligible because the flowrate required is relatively small for this system, see Appendix 7.

#### 4.2 Table of Relative Projected Annual Costs for different control systems and modes of aeration

The final results for the relative cost of aeration are as follows:

Mode of Aeration	Control System	Average aerator power (hp)	Projected annual cost (£)			Estimated Absolute Saving	Estimated Percentage Saving
			(av.) 1 aerator	Aeration lane	Total aeration		
Mechanical	none	12.5hp	£3080.71	£9242.13	£27,726.39	<u>N/A</u>	<u>N/A</u>
Mechanical	On-Off (1 aerator)	11.15hp	£2733.66	£8200.98	£24,602.94	£3123.45	11.27%
Mechanical	On-Off (2 aerators)	10.81hp	£2671.58	£8014.73	£24,044.19	£3682.20	13.28%
Mechanical	On-Off (3 aerators)	10.81hp	£2671.58	£8014.73	£24,044.19	£3682.20	13.28%
Mechanical	PID	9.78hp	£2410.17	£7230.52	£21,691.56	£6034.83	21.77%
Mechanical	PID (max 12.5hp)	8.90hp	£2192.89	£6578.66	£19,735.98	£7990.41	28.82%
Diffused	None (Same O <sub>2</sub> requirement)	8.84hp	£2178.68	£6536.03	£19,608.10	£8118.29	29.28%
Diffused	None (Same O <sub>2</sub> transfer)	6.43hp	£1416.58	£4249.73	£12,749.19	£14977.20	54.02%
Diffused	PID	4.19hp	£1032.65	£3097.96	£9292.88	£18432.51	66.48%

### 4.3 Conclusion

The aim of this thesis was to investigate possible alternatives to the energy intensive use of old inefficient mechanical aerators in the Activated Sludge Process at the Perth Wastewater Treatment plant. The ASM1 model was used with the software programme MATLAB/Simulink.

The initial conclusion that can be drawn on the effectiveness of this approach is that it can offer some insight into the process and provide an estimate of the power and cost of possible replacement aeration systems. The control systems that were suggested gave an idea of how the process could be controlled to a reasonable degree although in practice more advanced systems would be used.

The constraints of the ASM model were immediately realised in Chapter 2, when telemetry data from the plant was used as the process influent in the model. This initial run resulted in an extremely low DO concentration in the tank. From mass balance calculations it was subsequently discovered that the telemetry data represented influent flow of around 2 times the dry weather flow (DWF).

It can therefore be concluded that the ASM1 model is not tractable for wet weather flow, and that the huge inflow disturbances associated with municipal waste water treatment have an unrealistic effect on the DO concentrations in the simulated process. In order to continue the study, the telemetry data was scaled down such that the average flow equalled the estimated steady state DWF given in plant literature. After this, the modelled DO concentration matched the telemetry DO data to an acceptable degree. Although it was decided that the ASM1 models suitability was limited for wet weather flow, this does not mean that in reality the process cannot be controlled, rather that the description of the process in the simulation was inadequate. A PID controller could still be utilised for the control of DO concentration at the plant. A number of assumptions were also made before the simulation of the plant could take place, primarily that the aeration “leg” or plug flow bioreactor can be considered three ASM1 models in series each with an input of 12.5hp initially. It was discovered that there was a significant oxygen gradient along the length of the tank. Water Pollution Control (Larsen, 1998) states that such a dissolved oxygen gradient can be assumed, however the assumption that the tank can be divided into three separate compartments may have exaggerated this. If the DO levels are as low at the

influent end of the tank as the values in the simulation, a PID controller would be useful to increase the oxygen transfer in this area. If the DO gradient is more constant than the values in the simulation then the aeration cost associated with the controlled process will be slightly less. Since the DO sensors are located at the effluent end of the tank, there is no certainty that such an oxygen gradient does not exist.

From the simulation results, On-Off control can be concluded to be an unstable and unpredictable control algorithm, which is unsuitable for the control of the highly complex activated sludge process. The relatively fast dynamic response of the activated sludge system mean that as an aerator is turned off, the DO level in the tank falls dramatically according to the oxygen uptake rate (OUR) of the biomass in the tank. There can be seen to be a dynamic equilibrium between the addition of oxygen by aeration and its removal for substrate utilisation by the bacterial population. Oxygen is constantly driven into the sludge liquor by agitation and it is taken out of solution at the same rate during steady state conditions. According to the model, the OUR is sufficiently great to result in oxygen starvation during the “off” periods. The model does not take into account the slowing of the agitator as the power is turned off, where the system is still being supplied oxygen at a reduced rate, or the build up of the oxygen supply when the aerator is turned back on and the aerator revolutions increase. However great an effect this has on the stability of the system, it cannot change the nature of the On-Off controller response which is inherently cyclic and unstable. A further disadvantage of this method of control is the likelihood of increased stress on the aerators themselves as they are switched on and off. As discussed earlier, the control is improved, up to an optimum level, by the increase in possible switching frequency. If this frequency is increased, however, the risk of causing damage to the aerators also increases. It could be concluded that if no variable speed drives are fitted, it is better to leave the aerators running at full power.

It was discovered that PID control, or in this case PI control, was suitable for the activated sludge process as described in the ASM model.

Finally, the costs of energy consumption were estimated for several modes of aeration and control systems. The results, listed in the previous section, show that diffused aeration is less energy intensive than mechanical aeration, and that implantation of a good control system can yield a further energy saving. These costs would have to be considered with the cost of any changes to the current system. Because of the



differences in cost of different aeration systems, control equipment and final control elements and valves, the probable cost of replacement equipment was not considered.

#### 4.4 Further Work

If a more accurate estimation was needed of the viability of control systems and relative cost of replacement aeration systems at the Perth WWT plant, the following additional work could be carried out.

- Carry out experiments to calculate more accurately the  $kLa$  value, using information from the aerator manufacturer's data on oxygen transfer.
- Investigate the performance of more advanced activated sludge models with wet weather flow.
- Look into designing better control systems.
- Search for the cheapest and most effective diffused aerator and determine the pay back period of investment.

## Appendix 1

Table of components or states and their corresponding units

State Variable Description	State symbol	Units
Soluble inert organic matter	$S_I$	$\text{g COD m}^{-3}$
Readily biodegradable substrate	$S_I$	$\text{g COD m}^{-3}$
Particulate inert organic matter	$X_I$	$\text{g COD m}^{-3}$
Slowly biodegradable substrate	$X_S$	$\text{g COD m}^{-3}$
Active heterotrophic biomass	$X_{B,H}$	$\text{g COD m}^{-3}$
Active autotrophic biomass	$X_{B,A}$	$\text{g COD m}^{-3}$
Particulate products resulting from biomass decay	$X_P$	$\text{g COD m}^{-3}$
Oxygen	$S_O$	$\text{g COD m}^{-3}$
Nitrate and nitrate nitrogen	$S_{NO}$	$\text{g N m}^{-3}$
$\text{NH}_4^+$ and $\text{NH}_3$ nitrogen	$S_{NH}$	$\text{g N m}^{-3}$
Soluble biodegradable organic nitrogen	$S_{ND}$	$\text{g N m}^{-3}$
Particulate biodegradable organic nitrogen	$X_{ND}$	$\text{g N m}^{-3}$
Alkalinity	$S_{ALK}$	$\text{mol L}^{-1}$

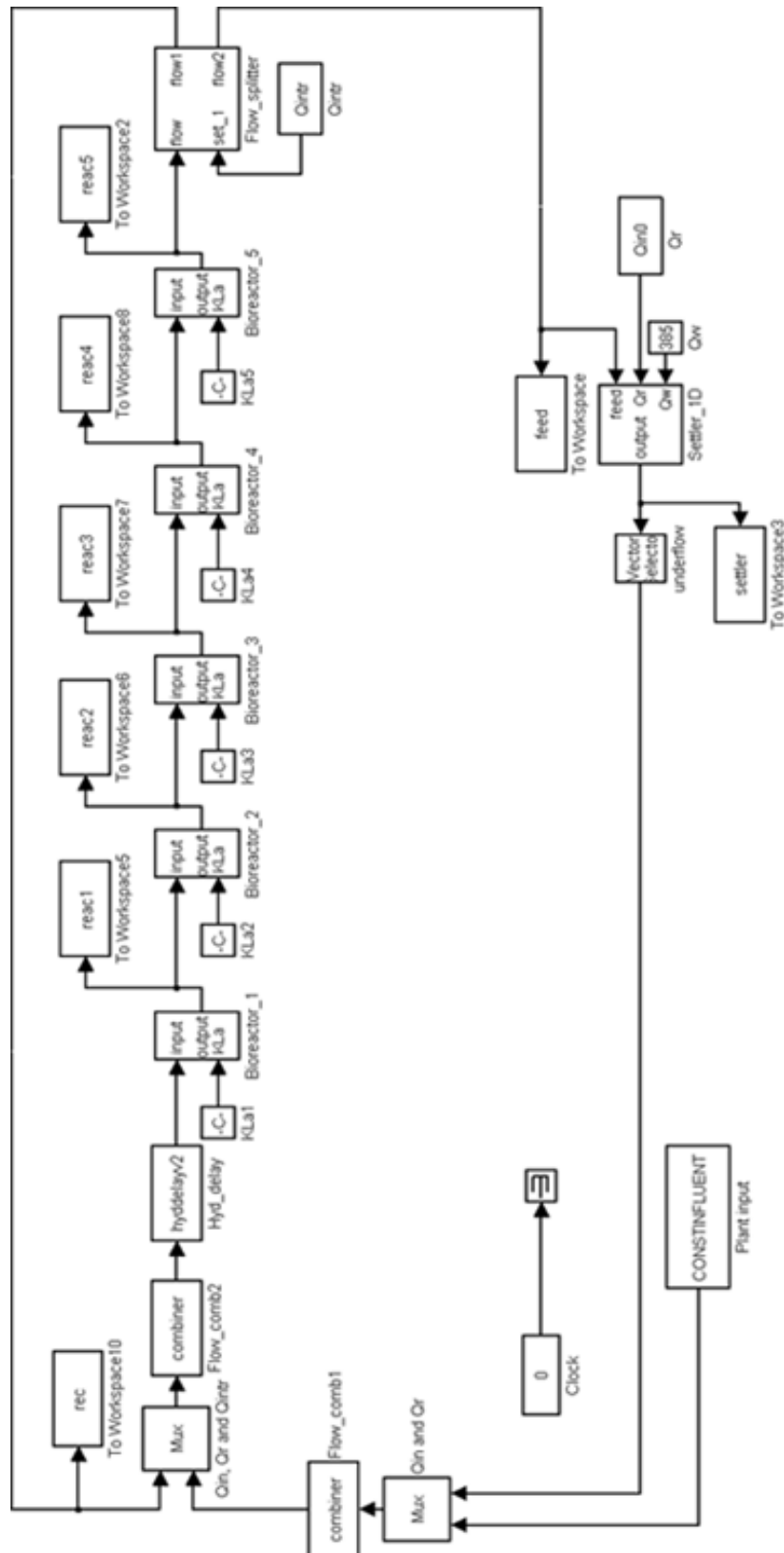
Table A1: State Values, notation and units.

Appendix 2 – Matrix representation of ASM 1 model

Process kinetics and stoichiometry for carbon oxidation, nitrification, and denitrification

Component $\rightarrow$	$i$	$j$ Process $\downarrow$	1	2	3	4	5	6	7	8	9	10	11	12	13	Process Rate, $\rho_j$ [ $ML^{-3}T^{-1}$ ]
Stoichiometric Parameters: Heterotrophic yield: $Y_H$ Autotrophic yield: $Y_A$ Fraction of biomass yielding particulate products: $f_P$ Mass N/Mass COD in biomass: $f_{NA}$ Mass N/Mass COD in products from biomass: $f_{NP}$	1	1	$S_i$	$S_s$	$X_i$	$X_s$	$X_{b,H}$	$X_{b,A}$	$X_p$	$S_o$	$S_{NO}$	$S_{NH}$	$S_{ND}$	$X_{ND}$	$S_{ALK}$	$\mu_H \left( \frac{S_s}{K_s + S_s} \right) \left( \frac{S_o}{K_{O,H} + S_o} \right) X_{b,H}$
	2	2	$S_i$	$S_s$	$X_i$	$X_s$	$X_{b,H}$	$X_{b,A}$	$X_p$	$S_o$	$S_{NO}$	$S_{NH}$	$S_{ND}$	$X_{ND}$	$S_{ALK}$	$\mu_H \left( \frac{S_s}{K_s + S_s} \right) \left( \frac{K_{O,H}}{K_{O,H} + S_o} \right) \times \left( \frac{S_{NO}}{K_{NO} + S_{NO}} \right) \eta_F X_{b,H}$
Observed Conversion Rates [ $ML^{-3}T^{-1}$ ]	3	3	$S_i$	$S_s$	$X_i$	$X_s$	$X_{b,H}$	$X_{b,A}$	$X_p$	$S_o$	$S_{NO}$	$S_{NH}$	$S_{ND}$	$X_{ND}$	$S_{ALK}$	$\mu_A \left( \frac{S_{NH}}{K_{NH} + S_{NH}} \right) \left( \frac{S_o}{K_{O,A} + S_o} \right) X_{b,A}$
	4	4	$S_i$	$S_s$	$X_i$	$X_s$	$X_{b,H}$	$X_{b,A}$	$X_p$	$S_o$	$S_{NO}$	$S_{NH}$	$S_{ND}$	$X_{ND}$	$S_{ALK}$	$b_H X_{b,H}$
Kinetic Parameters: Heterotrophic growth and decay: $\mu_H, K_s, K_{O,H}, K_{NO}, b_H$ Autotrophic growth and decay: $\mu_A, K_{NH}, K_{O,A}, b_A$ Correction factor for anoxic growth of heterotrophs: $\eta_F$ Ammonification: $k_A$ Hydrolysis: $k_h, K_X$ Correction factor for anoxic hydrolysis: $\eta_h$	5	5	$S_i$	$S_s$	$X_i$	$X_s$	$X_{b,H}$	$X_{b,A}$	$X_p$	$S_o$	$S_{NO}$	$S_{NH}$	$S_{ND}$	$X_{ND}$	$S_{ALK}$	$b_A X_{b,A}$
	6	6	$S_i$	$S_s$	$X_i$	$X_s$	$X_{b,H}$	$X_{b,A}$	$X_p$	$S_o$	$S_{NO}$	$S_{NH}$	$S_{ND}$	$X_{ND}$	$S_{ALK}$	$k_A S_{NO} X_{b,H}$
Soluble inert organic matter [ $ML^{-3}$ ]	7	7	$S_i$	$S_s$	$X_i$	$X_s$	$X_{b,H}$	$X_{b,A}$	$X_p$	$S_o$	$S_{NO}$	$S_{NH}$	$S_{ND}$	$X_{ND}$	$S_{ALK}$	$k_h \left( \frac{X_s}{K_X + (X_s/X_{b,H})} \right) \left( \frac{S_o}{K_{O,H} + S_o} \right) + \eta_h \left( \frac{K_{O,H}}{K_{O,H} + S_o} \right) \left( \frac{S_{NO}}{K_{NO} + S_{NO}} \right) X_{b,H}$
	8	8	$S_i$	$S_s$	$X_i$	$X_s$	$X_{b,H}$	$X_{b,A}$	$X_p$	$S_o$	$S_{NO}$	$S_{NH}$	$S_{ND}$	$X_{ND}$	$S_{ALK}$	$\rho_j (X_{ND}/X_s)$
Alkalinity – Molar units																
Particulate biodegradable organic nitrogen [ $M(N)L^{-3}$ ]																
Soluble biodegradable organic nitrogen [ $M(N)L^{-3}$ ]																
$NH_4^+$ + $NH_3$ nitrogen [ $M(N)L^{-3}$ ]																
Nitrate and nitrite nitrogen [ $M(N)L^{-3}$ ]																
Oxygen (negative COD) [ $M(COD)L^{-3}$ ]																
Particulate products arising from biomass decay [ $M(COD)L^{-3}$ ]																
Active autotrophic biomass [ $M(COD)L^{-3}$ ]																
Active heterotrophic biomass [ $M(COD)L^{-3}$ ]																
Slowly biodegradable substrate [ $M(COD)L^{-3}$ ]																
Particulate inert organic matter [ $M(COD)L^{-3}$ ]																
Readily biodegradable substrate [ $M(COD)L^{-3}$ ]																
Soluble inert organic matter [ $M(COD)L^{-3}$ ]																

Appendix 3 – Simulink flow diagram of COST simulation Benchmark.



#### Appendix 4 – Assumed influent composition, constant flow

State Variable Description	State symbol	Value (*1.0e+004)
Time	T	0
Soluble inert organic matter	S <sub>I</sub>	30.000g COD m <sup>-3</sup>
Readily biodegradable substrate	S <sub>I</sub>	63.634g COD m <sup>-3</sup>
Particulate inert organic matter	X <sub>I</sub>	58.476g COD m <sup>-3</sup>
Slowly biodegradable substrate	X <sub>S</sub>	224.35g COD m <sup>-3</sup>
Active heterotrophic biomass	X <sub>B,H</sub>	31.425g COD m <sup>-3</sup>
Active autotrophic biomass	X <sub>B,A</sub>	0g COD m <sup>-3</sup>
Particulate products resulting from biomass decay	X <sub>P</sub>	0g COD m <sup>-3</sup>
Oxygen	S <sub>O</sub>	0g COD m <sup>-3</sup>
Nitrate and nitrate nitrogen	S <sub>NO</sub>	0g N m <sup>-3</sup>
NH <sub>4</sub> <sup>+</sup> and NH <sub>3</sub> nitrogen	S <sub>NH</sub>	30.248g N m <sup>-3</sup>
Soluble biodegradable organic nitrogen	S <sub>ND</sub>	6.363g N m <sup>-3</sup>
Particulate biodegradable organic nitrogen	X <sub>ND</sub>	11.814g N m <sup>-3</sup>
Alkalinity	S <sub>ALK</sub>	7.000mol L <sup>-1</sup>
Total suspended solids	T <sub>SS</sub>	235.689g COD m <sup>-3</sup>
Volumetric Flowrate	Q	21477m <sup>3</sup> /day

## Appendix 4a – MATLAB programme “normalization”

```
1. innew=DRYINFLUENT(1,2:14);
2. xtotal=0;
3. for i=1:13,
4. xtotal=innew(i)+xtotal;
5. end
6. for i=1:13,
7. xpercentage(i)=innew(i)/xtotal;
8. end
9. filtimeaerflow1=filtimeaerflow1';
10. flow=filtimeaerflow1(:,2)*3600*24/1000;

11. [m n]=size(flow);

12. for i=1:m,
13. newxtotal(i)=flow(i)/21477*xtotal;
14. end

15. newconcentration=newxtotal'*xpercentage;

16. newtss=0.5*(newconcentration(:,3)+newconcentration(:,4)+newconcentration(
    :,5)+newconcentration(:,6)+newconcentration(:,7));

17. newinflow=[filtimeaerflow1(:,1) newconcentration newtss flow];
```



## Appendix 6 – Kinetic Parameters.

Parameter Description	Parameter symbol	S file notation	Value	Units
Maximum heterotrophic growth rate	$\mu_{mH}$	mu_H	4.0	day <sup>-1</sup>
Half Saturation (heterotrophic growth)	$K_S$	K_S	10.0	g COD m <sup>-3</sup>
Half Saturation (heterotrophic oxygen)	$K_{OH}$	K_OH	0.2	g O <sub>2</sub> m <sup>-3</sup>
Half Saturation (nitrate)	$K_{NO}$	K_NO	0.5	g NO <sub>3</sub> -N m <sup>-3</sup>
Heterotrophic Decay Rate	$b_H$	b_H	0.3	day <sup>-1</sup>
Anoxic Growth Rate correction factor	$\eta_g$	ny_g	0.8	dimensionless
Anoxic Hydrolysis Rate correction factor	$\eta_h$	ny_h	0.8	dimensionless
Maximum specific Hydrolysis Rate	$K_h$	k_h	3.0	gXS(XB, HCODday) <sup>-1</sup>
Half-Saturation (hydrolysis)	$K_X$	K_X	0.1	g XS(XB, HCOD) <sup>-1</sup>
Maximum autotrophic growth rate	$\mu_{mA}$	mu_A	0.5	day <sup>-1</sup>
Half-Saturation (auto-growth)	$K_{NH}$	K_NH	1.0	g NH <sub>3</sub> -N m <sup>-3</sup>
Autotrophic Decay Rate	$b_A$	k_a	0.05	day <sup>-1</sup>
Half-Saturation (auto-oxygen)	$K_{OA}$	K_OA	0.4	g O <sub>2</sub> m <sup>-3</sup>



## Appendix 7 – Calculation of head loss due to piping in diffused aeration

Friction losses can be calculated using the Darcy-Weisbach equation, thus:

$$h_L = f \frac{L}{D} h_i$$

where  $h_L$  = friction loss in inches of water.  
 $f$  = dimensionless friction factor  
 $L/D$  = length to diameter ratio of piping  
 $h_i$  = velocity head of air, inches of water

Some assumptions must be made here in order to derive a rough estimation for the additional power requirement.

The equivalent air flowrate is 9187.56m<sup>3</sup>/day, corresponding to a flowrate of 225.35ft<sup>3</sup>/min.

e.g  $9187.56\text{m}^3/\text{day} * \frac{3.281^2}{1} * \frac{1(\text{day})}{60 * 24(\text{min})}$

Table 10-7, Metcalf and Eddy gives “Typical information on the oxygen transfer efficiency of various systems”

A value can be assumed, for ceramic dome diffusers, of 1.5ft<sup>3</sup>/min.

$$\text{Therefore number of diffusers} = \frac{225.35\text{ft}^3/\text{min}}{1.5\text{ft}^3/\text{min}} = 150\text{diffusers}$$

Arranged along the bottom of the tank in, say, 5 rows.

Therefore, there are 30 aerators per row, and for each compartment,

$$10.7\text{m} * 5 = 53.5\text{m of piping inside the tank, assuming single pass.}$$

Adding another 25m, from the blowers to the tank itself, a rough estimate, e.g. 78.5m of piping, and assuming pipe diameter of 8inches. So 78.5m = 257.56ft

### Computation of head loss due to piping.

The theoretical adiabatic temperature rise during compression is given by Metcalf and Eddy as:

$$\Delta T_{ad} = \frac{T_1}{n} \left[ \left( \frac{P_2}{P_1} \right)^{0.283} - 1 \right]$$

where  $\Delta T_{ad}$  is the adiabatic temperature rise R (K)

so ambient air temperature is 20°C or 293K.

$$\Delta T_{ad} = \frac{293}{0.80} [(1.6)^{0.283} - 1]$$

$$\Delta T_{ad} = \underline{52^\circ\text{C}}$$

Therefore new temperature:  $T_2 = 52 + 20 = 72^\circ\text{C}$

Assuming the average temperature in the pipe is about 46°C.

Approximation of the air viscosity for temperature in Fahrenheit is given as:

$$\mu \text{ (centipoises)} = (161 + 0.28*(t)) * 10^{-4}$$

$$\mu \text{ (centipoises)} = (161 + 0.28(161.6)) * 10^{-4}$$

$$\mu \text{ (centipoises)} = \underline{193.2*10^{-4}}$$

The friction factor is calculated by a Moody diagram (Metcalf and Eddy, Appendix I)

Reynolds Number given by  $\frac{\rho v d}{\mu}$  or  $\text{Re} = \frac{28.4 * q_s}{d \mu}$ , where  $q_s$  is the flowrate

(225.35ft<sup>3</sup>/min) in the pipe, under prevailing temperature and conditions. D is the internal diameter, 8 inches and the viscosity,  $\mu$ , is in centipoises.

$$\text{Re} = \frac{28.4 * 225.35}{4 * 193 * 10^{-4}}$$

$$\text{Re} = \underline{8.28*10^4}$$

Therefore from the Moody diagram in Appendix I, Metcalf and Eddy, the dimensionless friction factor is 0.019.

$$\underline{f = 0.019}$$

Adding 10% design f = 0.0209

The volumetric flow in pipe is given by:

$$\frac{P_1 V_1}{T_1} = \frac{P_2 V_2}{T_2}$$

$$\frac{14.7 \text{ lb/in}^2 * 225.35 \text{ ft}^3 / \text{min}}{293} = \frac{(14.7 \text{ lb/in}^2 + 8 \text{ lb/in}^2) * V_2 \text{ ft}^3 / \text{min}}{319}$$

$$\underline{V_2 = 158.90 \text{ ft}^3 / \text{min}}$$

So assuming a pipe diameter of 2 inches:

$$v = \frac{V_2}{\frac{\pi * d^2}{4}}$$

where pipe internal diameter is 4/12feet.

$$v = \frac{158.90}{\frac{\pi \left(\frac{2}{12}\right)^2}{4}} = \frac{158.90}{0.0873} = 1820.86 \text{ ft} / \text{min}$$

Equivalent to 9.25m/s, a reasonable pipe velocity for a compressible fluid.

The specific weight of air is given at 22.7lb/in<sup>2</sup> and 115F by:

$$\gamma_a = \frac{P}{RT}$$

where

$$R = 53.3 \text{ ft.lb} / (\text{lb.air})^\circ R$$

$$\gamma_a = \frac{22.7(\text{lb} / \text{in}^2) * 144 \text{in}^2 / \text{ft}^2}{[53.3 \text{ ft.lb} / (\text{lb.air})^\circ R][(460 + 115)^\circ R]}$$

$$\gamma_a = \underline{0.107 \text{ lb} / \text{ft}^3}$$

One velocity head is given, in inches of water by:

$$h_i = \left(\frac{v}{1096}\right)^2 \gamma_a$$

$$h_i = \left(\frac{1820.86}{1096}\right)^2 0.107$$

$$\underline{h_i = 0.295 \text{ in water}}$$

The Darcy-Weisbach equation gives:

$$h_L = f \frac{L}{D} h_i$$

$$h_L = 0.0209 \frac{257.56}{0.667} 0.295$$

$$\underline{h_L = 2.383 \text{ in water}}$$

Equivalent to

$$\underline{h_L = 0.0861 \text{ lb} / \text{in}^2}$$

This pressure loss, which has to be overcome by the blower in order to supply the given oxygen requirement, is very low, compared to 8psi, the discharge pressure of the blower for the given flowrate. It is not high enough to have any significant effect on the power requirement according to Metcalf and Eddy, chapter 10, page 567 therefore, pressure losses due to piping can be taken as negligible.

## Appendix 8 – ASM1 C file S function

ASM1 is a C-file S-function for IAWQ AS Model No 1.

```
*
*/

#define S_FUNCTION_NAME asm1

#include "simstruc.h"
#include <math.h>

#define XINIT  ssGetArg(S,0)
#define PAR    ssGetArg(S,1)
#define V      ssGetArg(S,2)
#define SOSAT  ssGetArg(S,3)

/*
 * mdlInitializeSizes - initialize the sizes array
 */
static void mdlInitializeSizes(SimStruct *S)
{
    ssSetNumContStates( S, 13); /*13 number of continuous states */
    ssSetNumDiscStates( S, 0); /* number of discrete states */
    ssSetNumInputs(     S, 16); /* number of inputs */
    ssSetNumOutputs(    S, 15); /* number of outputs */
    ssSetDirectFeedThrough(S, 1); /* direct feedthrough flag */
    ssSetNumSampleTimes( S, 1); /* number of sample times */
    ssSetNumSFcnParams(  S, 4); /* number of input arguments */
    ssSetNumRWork(      S, 0); /* number of real work vector elements */
    ssSetNumIWork(      S, 0); /* number of integer work vector elements*/
    ssSetNumPWork(      S, 0); /* number of pointer work vector elements*/
}

/*
 * mdlInitializeSampleTimes - initialize the sample times array
 */
static void mdlInitializeSampleTimes(SimStruct *S)
{
    ssSetSampleTime(S, 0, CONTINUOUS_SAMPLE_TIME);
    ssSetOffsetTime(S, 0, 0.0);
}

/*
 * mdlInitializeConditions - initialize the states
 */
static void mdlInitializeConditions(double *x0, SimStruct *S)
{
    int i;
```

```

for (i = 0; i < 13; i++) {
    x0[i] = mxGetPr(XINIT)[i];
}
}

/*
 * mdlOutputs - compute the outputs
 */

static void mdlOutputs(double *y, double *x, double *u, SimStruct *S, int tid)
{
    double X_I2TSS, X_S2TSS, X_BH2TSS, X_BA2TSS, X_P2TSS;
    int i;

    X_I2TSS = mxGetPr(PAR)[19];
    X_S2TSS = mxGetPr(PAR)[20];
    X_BH2TSS = mxGetPr(PAR)[21];
    X_BA2TSS = mxGetPr(PAR)[22];
    X_P2TSS = mxGetPr(PAR)[23];

    for (i = 0; i < 13; i++) {
        y[i] = x[i];
    }

    y[13]=X_I2TSS*x[2]+X_S2TSS*x[3]+X_BH2TSS*x[4]+X_BA2TSS*x[5]+X_P2TS
    S*x[6];
    y[14]=u[14]; /* x[13] */

}

/*
 * mdlUpdate - perform action at major integration time step
 */

static void mdlUpdate(double *x, double *u, SimStruct *S, int tid)
{
}

/*
 * mdlDerivatives - compute the derivatives
 */

static void mdlDerivatives(double *dx, double *x, double *u, SimStruct *S, int tid)
{
    double mu_H, K_S, K_OH, K_NO, b_H, mu_A, K_NH, K_OA, b_A, ny_g, k_a, k_h,
    K_X, ny_h;
    double Y_H, Y_A, f_P, i_XB, i_XP;
    double proc1, proc2, proc3, proc4, proc5, proc6, proc7, proc8, proc3x;

```

```

double reac1, reac2, reac3, reac4, reac5, reac6, reac7, reac8, reac9, reac10, reac11,
reac12, reac13;
double vol, SO_sat, T;
double xtemp[13];
int i;

mu_H = mxGetPr(PAR)[0];
K_S = mxGetPr(PAR)[1];
K_OH = mxGetPr(PAR)[2];
K_NO = mxGetPr(PAR)[3];
b_H = mxGetPr(PAR)[4];
mu_A = mxGetPr(PAR)[5];
K_NH = mxGetPr(PAR)[6];
K_OA = mxGetPr(PAR)[7];
b_A = mxGetPr(PAR)[8];
ny_g = mxGetPr(PAR)[9];
k_a = mxGetPr(PAR)[10];
k_h = mxGetPr(PAR)[11];
K_X = mxGetPr(PAR)[12];
ny_h = mxGetPr(PAR)[13];
Y_H = mxGetPr(PAR)[14];
Y_A = mxGetPr(PAR)[15];
f_P = mxGetPr(PAR)[16];
i_XB = mxGetPr(PAR)[17];
i_XP = mxGetPr(PAR)[18];
vol = mxGetPr(V)[0];
SO_sat = mxGetPr(SOSAT)[0];

for (i = 0; i < 13; i++) {
    if (x[i] < 0)
        xtemp[i] = 0;
    else
        xtemp[i] = x[i];
}

if (u[15] < 0)
    x[7] = fabs(u[15]);

proc1 =
mu_H*(xtemp[1]/(K_S+xtemp[1]))*(xtemp[7]/(K_OH+xtemp[7]))*xtemp[4];
proc2 =
mu_H*(xtemp[1]/(K_S+xtemp[1]))*(K_OH/(K_OH+xtemp[7]))*(xtemp[8]/(K_NO+
xtemp[8]))*ny_g*xtemp[4];
proc3 =
mu_A*(xtemp[9]/(K_NH+xtemp[9]))*(xtemp[7]/(K_OA+xtemp[7]))*xtemp[5];
/* in GPS-X they use proc3x instead of proc3 in the oxygen equation */
/*
proc3x =
mu_A*(xtemp[9]/(K_NH+xtemp[9]))*(xtemp[7]/(K_OH+xtemp[7]))*xtemp[5]; */
proc4 = b_H*xtemp[4];
proc5 = b_A*xtemp[5];

```

```

proc6 = k_a*xtemp[10]*xtemp[4];
proc7 =
k_h*((xtemp[3]/xtemp[4])/(K_X+(xtemp[3]/xtemp[4])))*((xtemp[7]/(K_OH+xtemp[
7]))+ny_h*(K_OH/(K_OH+xtemp[7]))*(xtemp[8]/(K_NO+xtemp[8]))) *xtemp[4];
proc8 = proc7*xtemp[11]/xtemp[3];

reac1 = 0;
reac2 = (-proc1-proc2)/Y_H+proc7;
reac3 = 0;
reac4 = (1-f_P)*(proc4+proc5)-proc7;
reac5 = proc1+proc2-proc4;
reac6 = proc3-proc5;
reac7 = f_P*(proc4+proc5);
reac8 = -((1-Y_H)/Y_H)*proc1-((4.57-Y_A)/Y_A)*proc3;
reac9 = -((1-Y_H)/(2.86*Y_H))*proc2+proc3/Y_A;
reac10 = -i_XB*(proc1+proc2)-(i_XB+(1/Y_A))*proc3+proc6;
reac11 = -proc6+proc8;
reac12 = (i_XB-f_P*i_XP)*(proc4+proc5)-proc8;
reac13 = -i_XB/14*proc1+((1-Y_H)/(14*2.86*Y_H)-(i_XB/14))*proc2-
((i_XB/14)+1/(7*Y_A))*proc3+proc6/14;

dx[0] = 1/vol*(u[14]*(u[0]-x[0]))+reac1;
dx[1] = 1/vol*(u[14]*(u[1]-x[1]))+reac2;
dx[2] = 1/vol*(u[14]*(u[2]-x[2]))+reac3;
dx[3] = 1/vol*(u[14]*(u[3]-x[3]))+reac4;
dx[4] = 1/vol*(u[14]*(u[4]-x[4]))+reac5;
dx[5] = 1/vol*(u[14]*(u[5]-x[5]))+reac6;
dx[6] = 1/vol*(u[14]*(u[6]-x[6]))+reac7;
if (u[15] < 0)
    dx[7] = 0;
else
    dx[7] = 1/vol*(u[14]*(u[7]-x[7]))+reac8+u[15]*(SO_sat-x[7]);
dx[8] = 1/vol*(u[14]*(u[8]-x[8]))+reac9;
dx[9] = 1/vol*(u[14]*(u[9]-x[9]))+reac10;
dx[10] = 1/vol*(u[14]*(u[10]-x[10]))+reac11;
dx[11] = 1/vol*(u[14]*(u[11]-x[11]))+reac12;
dx[12] = 1/vol*(u[14]*(u[12]-x[12]))+reac13;
/*dx[13] = (u[14]-x[13])/T; low pass filter for flow, avoid algebraic loops */

}

/*
 * mdlTerminate - called when the simulation is terminated.
 */
static void mdlTerminate(SimStruct *S)
{
}

#ifdef MATLAB_MEX_FILE /* Is this file being compiled as a MEX-file? */

```

```
#include "simulink.c" /* MEX-file interface mechanism */  
#else  
#include "cg_sfun.h" /* Code generation registration function */  
#endif
```



## Appendix 9 – Combiner C file S function

```
* flowcombiner.c calculates the concentrations when adding two flow
* streams together.
*
*/

#define S_FUNCTION_NAME combiner

#include "simstruc.h"

/*
 * mdlInitializeSizes - initialize the sizes array
 */
static void mdlInitializeSizes(SimStruct *S)
{
    ssSetNumContStates( S, 0); /* number of continuous states */
    ssSetNumDiscStates( S, 0); /* number of discrete states */
    ssSetNumInputs( S, 30); /* number of inputs */
    ssSetNumOutputs( S, 15); /* number of outputs */
    ssSetDirectFeedThrough(S, 1); /* direct feedthrough flag */
    ssSetNumSampleTimes( S, 1); /* number of sample times */
    ssSetNumSFcnParams( S, 0); /* number of input arguments */
    ssSetNumRWork( S, 0); /* number of real work vector elements */
    ssSetNumIWork( S, 0); /* number of integer work vector elements*/
    ssSetNumPWork( S, 0); /* number of pointer work vector elements*/
}

/*
 * mdlInitializeSampleTimes - initialize the sample times array
 */
static void mdlInitializeSampleTimes(SimStruct *S)
{
    ssSetSampleTime(S, 0, CONTINUOUS_SAMPLE_TIME);
    ssSetOffsetTime(S, 0, 0.0);
}

/*
 * mdlInitializeConditions - initialize the states
 */
static void mdlInitializeConditions(double *x0, SimStruct *S)
{
}

/*
 * mdlOutputs - compute the outputs
 */
```

```

static void mdlOutputs(double *y, double *x, double *u, SimStruct *S, int tid)
{
    y[0]=(u[0]*u[14] + u[15]*u[29])/(u[14]+u[29]);
    y[1]=(u[1]*u[14] + u[16]*u[29])/(u[14]+u[29]);
    y[2]=(u[2]*u[14] + u[17]*u[29])/(u[14]+u[29]);
    y[3]=(u[3]*u[14] + u[18]*u[29])/(u[14]+u[29]);
    y[4]=(u[4]*u[14] + u[19]*u[29])/(u[14]+u[29]);
    y[5]=(u[5]*u[14] + u[20]*u[29])/(u[14]+u[29]);
    y[6]=(u[6]*u[14] + u[21]*u[29])/(u[14]+u[29]);
    y[7]=(u[7]*u[14] + u[22]*u[29])/(u[14]+u[29]);
    y[8]=(u[8]*u[14] + u[23]*u[29])/(u[14]+u[29]);
    y[9]=(u[9]*u[14] + u[24]*u[29])/(u[14]+u[29]);
    y[10]=(u[10]*u[14] + u[25]*u[29])/(u[14]+u[29]);
    y[11]=(u[11]*u[14] + u[26]*u[29])/(u[14]+u[29]);
    y[12]=(u[12]*u[14] + u[27]*u[29])/(u[14]+u[29]);
    y[13]=(u[13]*u[14] + u[28]*u[29])/(u[14]+u[29]);
    y[14]=(u[14]+u[29]);
}

/*
 * mdlUpdate - perform action at major integration time step
 */

static void mdlUpdate(double *x, double *u, SimStruct *S, int tid)
{
}

/*
 * mdlDerivatives - compute the derivatives
 */
static void mdlDerivatives(double *dx, double *x, double *u, SimStruct *S, int tid)
{
}

/*
 * mdlTerminate - called when the simulation is terminated.
 */
static void mdlTerminate(SimStruct *S)
{
}

#ifdef MATLAB_MEX_FILE /* Is this file being compiled as a MEX-file? */
#include "simulink.c" /* MEX-file interface mechanism */
#else
#include "cg_sfun.h" /* Code generation registration function */
#endif

```

## Appendix 10 – Hyd-delay C file S function

```
#define S_FUNCTION_NAME hyddelayv2

#include "simstruc.h"

#define XINIT  ssGetArg(S,0)
#define PAR    ssGetArg(S,1)
#define T      ssGetArg(S,2)

/*
 * mdlInitializeSizes - initialize the sizes array
 */
static void mdlInitializeSizes(SimStruct *S)
{
    ssSetNumContStates( S, 14); /*13 number of continuous states */
    ssSetNumDiscStates( S, 0); /* number of discrete states */
    ssSetNumInputs(     S, 15); /* number of inputs */
    ssSetNumOutputs(    S, 15); /* number of outputs */
    ssSetDirectFeedThrough(S, 0); /* direct feedthrough flag */
    ssSetNumSampleTimes( S, 1); /* number of sample times */
    ssSetNumSFcnParams(  S, 3); /* number of input arguments */
    ssSetNumRWork(       S, 0); /* number of real work vector elements */
    ssSetNumIWork(       S, 0); /* number of integer work vector elements*/
    ssSetNumPWork(       S, 0); /* number of pointer work vector elements*/
}

/*
 * mdlInitializeSampleTimes - initialize the sample times array
 */
static void mdlInitializeSampleTimes(SimStruct *S)
{
    ssSetSampleTime(S, 0, CONTINUOUS_SAMPLE_TIME);
    ssSetOffsetTime(S, 0, 0.0);
}

/*
 * mdlInitializeConditions - initialize the states
 */
static void mdlInitializeConditions(double *x0, SimStruct *S)
{
    int i;

    for (i = 0; i < 14; i++) {
        x0[i] = mxGetPr(XINIT)[i];
    }
}

/*
```

```

* mdlOutputs - compute the outputs
*/

static void mdlOutputs(double *y, double *x, double *u, SimStruct *S, int tid)
{
    double X_I2TSS, X_S2TSS, X_BH2TSS, X_BA2TSS, X_P2TSS;
    int i;

    X_I2TSS = mxGetPr(PAR)[19];
    X_S2TSS = mxGetPr(PAR)[20];
    X_BH2TSS = mxGetPr(PAR)[21];
    X_BA2TSS = mxGetPr(PAR)[22];
    X_P2TSS = mxGetPr(PAR)[23];

    for (i = 0; i < 13; i++) {
        y[i] = x[i]/x[13];
    }

    y[13]=(X_I2TSS*x[2]+X_S2TSS*x[3]+X_BH2TSS*x[4]+X_BA2TSS*x[5]+X_P2T
SS*x[6])/x[13];
    y[14]=x[13];
}

/*
* mdlUpdate - perform action at major integration time step
*/

static void mdlUpdate(double *x, double *u, SimStruct *S, int tid)
{
}

/*
* mdlDerivatives - compute the derivatives
*/

static void mdlDerivatives(double *dx, double *x, double *u, SimStruct *S, int tid)
{
    int i;
    double timeconst;

    timeconst = mxGetPr(T)[0];
    if (timeconst > 0.000001) {
        dx[0] = (u[0]*u[14]-x[0])/timeconst;
        dx[1] = (u[1]*u[14]-x[1])/timeconst;
        dx[2] = (u[2]*u[14]-x[2])/timeconst;
        dx[3] = (u[3]*u[14]-x[3])/timeconst;
        dx[4] = (u[4]*u[14]-x[4])/timeconst;
        dx[5] = (u[5]*u[14]-x[5])/timeconst;
        dx[6] = (u[6]*u[14]-x[6])/timeconst;
        dx[7] = (u[7]*u[14]-x[7])/timeconst;
    }
}

```

```

dx[8] = (u[8]*u[14]-x[8])/timeconst;
dx[9] = (u[9]*u[14]-x[9])/timeconst;
dx[10] = (u[10]*u[14]-x[10])/timeconst;
dx[11] = (u[11]*u[14]-x[11])/timeconst;
dx[12] = (u[12]*u[14]-x[12])/timeconst;
dx[13] = (u[14]-x[13])/timeconst; }
else {
dx[0] = 0;
dx[1] = 0;
dx[2] = 0;
dx[3] = 0;
dx[4] = 0;
dx[5] = 0;
dx[6] = 0;
dx[7] = 0;
dx[8] = 0;
dx[9] = 0;
dx[10] = 0;
dx[11] = 0;
dx[12] = 0;
dx[13] = 0;
x[0] = u[0]*u[14];
x[1] = u[1]*u[14];
x[2] = u[2]*u[14];
x[3] = u[3]*u[14];
x[4] = u[4]*u[14];
x[5] = u[5]*u[14];
x[6] = u[6]*u[14];
x[7] = u[7]*u[14];
x[8] = u[8]*u[14];
x[9] = u[9]*u[14];
x[10] = u[10]*u[14];
x[11] = u[11]*u[14];
x[12] = u[12]*u[14];
x[13] = u[14];
}
}

/*
 * mdlTerminate - called when the simulation is terminated.
 */
static void mdlTerminate(SimStruct *S)
{
}

#ifdef MATLAB_MEX_FILE /* Is this file being compiled as a MEX-file? */
#include "simulink.c" /* MEX-file interface mechanism */
#else
#include "cg_sfun.h" /* Code generation registration function */

```

## Bibliography

1. Wastewater Engineering, Treatment Disposal Reuse, Third Edition (Metcalf and Eddy)
2. The COST simulation benchmark, Description and Simulation Manual (COST action 624)
3. Energy in Wastewater Treatment (Owen)
4. Control Engineering, an introductory course (J Wilkie et al)
5. PID Controllers, Theory, Design and Tuning (K. Astrom)
6. Water Pollution Control (V Larsen)
7. Activated Sludge Models ASM1, ASM2, ASM2D and ASM3 (IAWQ task group on mathematical modelling for design and operation of biological wastewater treatment)
8. Perry's Chemical Engineers Handbook (Perry and Green)
9. Wastewater Treatment Systems (Modelling, Diagnosis and Control) (Olsson and Newell)
10. Control and Instrumentation for Wastewater Treatment Plants (Katebi et al)
11. Process Control (B Postlethwaite)
12. Biological Wastewater Treatment, Second Edition. (Leslie Grady Jnr et al)
13. Improvements in Modelling Dissolved Oxygen in Activated Sludge Systems (Makinia and Wells)
14. Notes on Project Work and Management (C. Kuo)
15. Perth Wastewater Treatment Plant (North of Scotland Water Authority)
16. Activated Sludge – Theory and Practice (N.F Gray)
17. Control and Estimation Strategies Applied to the Activated Sludge Process (C F Lindberg)



